Article

Current Biology

Skin mycobiota-mediated antagonism against *Staphylococcus aureus* through a modified fatty acid

Graphical abstract

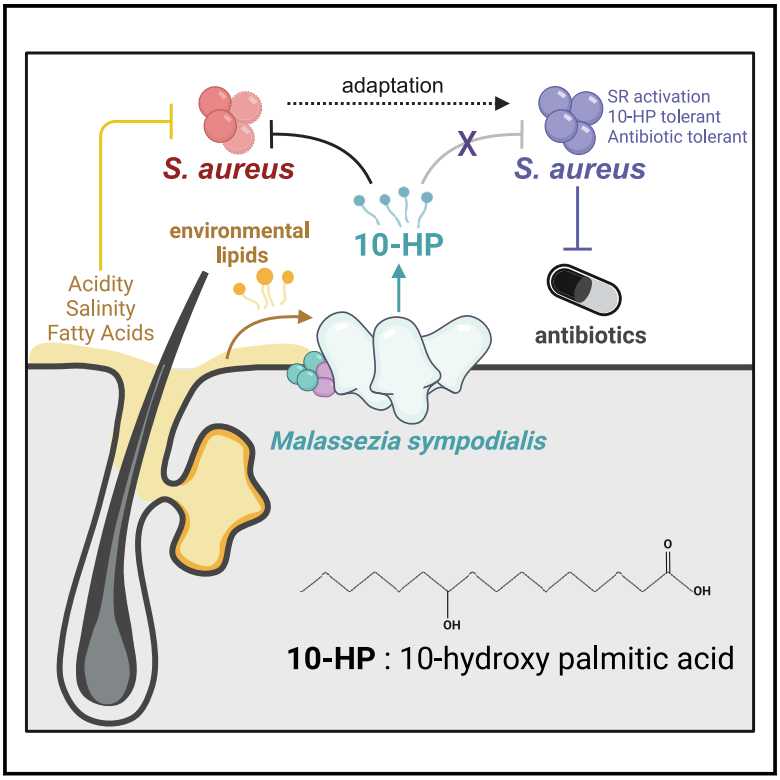

Authors

Caitlin H. Kowalski, Uyen Thy Nguyen, Susannah Lawhorn, ..., Won Se Suh, Lindsay Kalan, Matthew F. Barber

Correspondence

ckowalsk@uoregon.edu (C.H.K.), mfbarber@uoregon.edu (M.F.B.)

In brief

Kowalski et al. show that the skin-resident yeast *M. sympodialis* antagonizes *S. aureus* through generation of a hydroxyl fatty acid. *S. aureus* adapts to this antagonism by activating the stringent response, resulting in multidrug tolerance. This study highlights a role for fungi in colonization resistance, with consequences for antibiotic sensitivity.

Highlights

- *M. sympodialis* reduces *S. aureus* colonization on human skin
- *M. sympodialis* generates antimicrobial 10-hydroxy palmitic acid
- *S. aureus* adapts to *Malassezia* antagonism through stringent response activation
- Adaptation to *Malassezia* antagonism coincides with broad multidrug tolerance

Kowalski et al., 2025, Current Biology *35*, 1–16
May 19, 2025
https://doi.org/10.1016/j.cub.2025.03.055

CellPress

Please cite this article in press as: Kowalski et al., Skin mycobiota-mediated antagonism against *Staphylococcus aureus* through a modified fatty acid, Current Biology (2025), https://doi.org/10.1016/j.cub.2025.03.055

Current Biology

CellPress

Article

Skin mycobiota-mediated antagonism against *Staphylococcus aureus* through a modified fatty acid

Caitlin H. Kowalski,[1,*] Uyen Thy Nguyen,[2,4] Susannah Lawhorn,[5] T. Jarrod Smith,[5] Rebecca M. Corrigan,[6,7] Won Se Suh,[2,8] Lindsay Kalan,[2,3,8] and Matthew F. Barber[1,9,10,*]

[1]Institute of Ecology and Evolution, University of Oregon, Eugene, OR 97403, USA
[2]Department of Biochemistry and Biomedical Sciences, McMaster University, Hamilton, ON L8N 3Z5, Canada
[3]Department of Medical Microbiology and Immunology, School of Medicine and Public Health, University of Wisconsin-Madison, Madison, WI 53706, USA
[4]Microbiology Doctoral Training Program, University of Wisconsin-Madison, Madison, WI 53705, USA
[5]Institute of Molecular Biology, University of Oregon, Eugene, OR 97403, USA
[6]Florey Institute, School of Biosciences, University of Sheffield, Sheffield S10 2TN, UK
[7]The School of Medicine, University College Dublin, Belfield, Dublin 4, Dublin D04 V1W8, Ireland
[8]M.G. DeGroote Institute for Infectious Disease Research, David Braley Centre for Antibiotic Discovery, McMaster University, Hamilton, ON L8N 3Z5, Canada
[9]Department of Biology, University of Oregon, Eugene, OR 97403, USA
[10]Lead contact
*Correspondence: ckowalsk@uoregon.edu (C.H.K.), mfbarber@uoregon.edu (M.F.B.)
https://doi.org/10.1016/j.cub.2025.03.055

SUMMARY

Microbiota promote host health by inhibiting pathogen colonization, yet how host-resident fungi or mycobiota contribute to this process remains unclear. The human skin mycobiota is uniquely stable compared with other body sites and dominated by skin-adapted yeasts of the genus *Malassezia*. We observe that colonization of human skin by *Malassezia sympodialis* significantly reduces subsequent colonization by the prominent bacterial pathogen *Staphylococcus aureus*. *In vitro*, *M. sympodialis* generates a hydroxyl palmitic acid isomer from environmental sources that has potent bactericidal activity against *S. aureus* in the context of skin-relevant stressors and is sufficient to impair *S. aureus* skin colonization. Leveraging experimental evolution to pinpoint mechanisms of *S. aureus* adaptation in response to antagonism by *Malassezia*, we identified multiple mutations in the stringent response regulator Rel that promote survival against *M. sympodialis* and provide a competitive advantage on human skin when *M. sympodialis* is present. Similar Rel alleles have been reported in *S. aureus* clinical isolates, and natural Rel variants are sufficient for tolerance to *M. sympodialis* antagonism. Partial stringent response activation underlies tolerance to clinical antibiotics, with both laboratory-evolved and natural Rel variants conferring multidrug tolerance in a manner that is dependent on the alternative sigma factor SigB. These findings demonstrate the ability of the mycobiota to mediate pathogen colonization resistance through generation of a hydroxy palmitic acid isomer, identify new mechanisms of bacterial adaptation in response to microbiota antagonism, and reveal the potential for microbiota-driven evolution to shape pathogen antibiotic susceptibility.

INTRODUCTION

Staphylococcus aureus is the primary cause of skin and soft tissue infections, resulting in approximately 500,000 hospitalizations annually in the United States,[1] and in 2019 was associated with more than one million deaths globally.[2] Despite the ability of *S. aureus* to thrive within wounds and to colonize the nares, colonization of most healthy skin sites occurs transiently.[3,4] Features of healthy skin contribute to this colonization deficiency, including acidic pH, antimicrobial fatty acids, and host-produced antimicrobial peptides (AMPs).[5–7] Additionally, skin-resident bacteria inhibit pathogen colonization, a process referred to as colonization resistance.[8] Microbial factors inhibit *S. aureus* directly,[9,10] disrupt biofilm formation,[11] activate host defenses,[12] or modulate *S. aureus* virulence.[13,14] The application of a naturally antagonistic skin-resident bacteria is in clinical trials to treat *S. aureus* colonization in atopic dermatitis.[15]

Despite examples of bacteria-mediated colonization resistance,[8] and the critical need for novel antimicrobials,[16] little is known about how skin-resident fungi contribute to pathogen defense. Human skin contains a larger proportion of fungi compared with other body sites.[17,18] This skin mycobiota is largely dominated by a single genus of yeast, *Malassezia*.[19,20] Ubiquitous colonizers of mammalian skin, *Malassezia* are well-adapted to the dermal environment. They have some of the smallest genomes of free-living fungi, a characteristic of host

Please cite this article in press as: Kowalski et al., Skin mycobiota-mediated antagonism against *Staphylococcus aureus* through a modified fatty acid, Current Biology (2025), https://doi.org/10.1016/j.cub.2025.03.055

niche specialization.[21,22] They have horizontally acquired genetic material from skin-resident bacteria, which may contribute to niche-specific adaptation.[21,23] And, they have lost the ability to produce fatty acids *de novo* and are dependent on exogenous lipid sources, such as those abundant on skin.[21,24] As these yeasts likely adapted to colonize skin in the presence of other microbes, we hypothesized that *Malassezia* have evolved strategies to thrive in polymicrobial communities. Consistent with this hypothesis, *Malassezia globosa* secretes a protease capable of disrupting *S. aureus* biofilms,[25] and recent studies suggest a possible protective role for *Malassezia* against colonization by the fungal pathogen *Candida auris*.[26,27] Beyond these examples, it is unknown whether *Malassezia* produce other antimicrobial effectors capable of inhibiting bacterial colonization or how pathogens adapt to antagonists within the microbiota.

Here, we use human skin biopsies from healthy donors and *in vitro* host-like conditions to investigate the ability of *Malassezia* to inhibit *S. aureus* growth and skin colonization. We further investigate the potential for microbiota antagonism to shape pathogen evolution by selecting for tolerance in *S. aureus* exposed to *Malassezia* antimicrobial products. We report that *Malassezia sympodialis* antagonizes *S. aureus* through generation of 10-hydroxy palmitic acid (10-HP). Long-term exposure to *M. sympodialis* antagonism selects for heritable tolerance in *S. aureus* through activation of the stringent response (SR) that concomitantly results in tolerance to clinical antibiotics. This work proposes that skin-resident fungi contribute to colonization resistance by transforming environmental lipids to antimicrobial hydroxy fatty acids, highlighting the important role that often-overlooked fungi play at the interface of the microbiota and host health. Furthermore, our findings illustrate the potential for intermicrobial antagonism to shape pathogen evolution, with consequences for antibiotic susceptibility.

RESULTS

M. sympodialis inhibits *S. aureus* growth *in vitro*

To determine whether *Malassezia* can alter *S. aureus* growth, we selected a clinical isolate of *S. aureus*, NRS193, as our wild-type (WT) strain. This community-associated, methicillin-resistant *S. aureus* (CA-MRSA) strain was selected because it is closely related to the reference strain MW2, is not laboratory adapted, and did not originate from a skin infection.[28] We inoculated NRS193 adjacent to 72 h colonies of *M. sympodialis*, *Malassezia furfur*, or *Malassezia pachydermatis* grown on mDixon. This media is used to culture fastidious *Malassezia* and recapitulates the lipid-rich skin environment. After 24 h, only *M. sympodialis* inhibited *S. aureus* growth (Figure 1A). *M. sympodialis* is one of the three most prevalent *Malassezia* species on healthy human skin, whereas *M. furfur* is less prevalent but more easily culturable.[21] *M. pachydermatis* commonly colonizes non-human mammals.[29] *M. sympodialis* did not impact growth of *Escherichia coli* or the skin commensal *Staphylococcus hominis* (Figure 1B). To determine whether *Malassezia* impacts *S. aureus* growth when inoculated simultaneously, we established mixed colony biofilms on mDixon of *S. aureus* with *M. sympodialis*, *M. furfur*, or *M. pachydermatis*. Only co-culture with *M. sympodialis* significantly reduced *S. aureus* recovery compared with *S. aureus* monoculture after 6 days (Figure 1C). Similar results were observed with modified potato dextrose agar (mPDA)[30] (Figure S1A). Collectively, we conclude that *M. sympodialis* can antagonize *S. aureus in vitro*.

M. sympodialis inhibits *S. aureus* colonization of human skin

We hypothesized that *M. sympodialis* colonization of human skin would reduce subsequent *S. aureus* colonization. Human skin biopsies are used to study host-microbe interactions, including host-*Malassezia* interactions.[31–33] These biopsies are viable, full-thickness human skin that contain skin appendages and tissue-resident leukocytes.[32] Presurgical sterilization abolishes the existing microbiome, as plating on non-selective media showed no microbial growth. We inoculated biopsies, prepared from abdominal skin of four donors, with *M. sympodialis* or the vehicle PBS (Figure 1D). *M. sympodialis* was labeled with a cell wall stain to visualize colonization (Figures 1E and S1B). 6 days after *M. sympodialis* or PBS inoculation, all biopsies were inoculated with *S. aureus*-expressing GFP. After 24 h of *S. aureus* colonization, biopsies were physically disrupted to remove *S. aureus*. Biopsies pre-colonized with *M. sympodialis* had significantly less *S. aureus* colonization compared with biopsies with PBS (Figures 1F and 1G). These findings suggest, consistent with our *in vitro* observations, that *M. sympodialis* antagonizes *S. aureus* on skin.

M. sympodialis produces potent bactericidal products active against *S. aureus*

Skin-resident bacteria secrete antimicrobial compounds capable of inhibiting *S. aureus* growth[9,10,15,34] and reducing virulence.[13,14] Initial *in vitro* experiments suggest the *M. sympodialis* antimicrobial effector is extracellular (Figure 1A). To confirm this, we grew *M. sympodialis* in monoculture and collected cell-free supernatant (CFS) after 96 h. Compared with pH-matched media controls, *M. sympodialis*-CFS from mDixon showed dose-dependent antimicrobial activity against *S. aureus* after 2 h (Figure 2A), with ~1,000-fold reduction in viability with 50% *M. sympodialis*-CFS. When *M. sympodialis* is grown in modified potato dextrose broth (mPDB) or synthetic sebum media, a 24 h *M. sympodialis*-CFS treatment reduces *S. aureus* colony-forming units (CFUs) by 1,000-fold relative to controls (Figures S1C and S1D). This suggests that media components can alter antimicrobial production or exacerbate *in vitro* potency.

We opted to continue with *M. sympodialis*-CFS prepared from mDixon and monitored antibacterial activity of 50% *M. sympodialis*-CFS over 24 h with four *S. aureus* strains. With two methicillin-sensitive (MSSA) and two methicillin-resistant (MRSA) *S. aureus* strains, we observed rapid killing during the first 2 h of 50% *M. sympodialis*-CFS treatment (100- to 1,000-fold reduction), followed by a gradual reduction in viability from 2 to 24 h (Figure 2B). We observed no *S. aureus* growth in pH-matched media (pH 5.5) over 24 h, despite *S. aureus* growing in mDixon at pH 6 (Figure S1E). Because we observed reproducible, rapid killing in the first 2 h of treatment, we selected 2 h treatment with 50% *M. sympodialis*-CFS for future experiments.

We next assessed whether *M. sympodialis*-CFS can reduce *S. aureus* colonization on human skin. We inoculated human

Please cite this article in press as: Kowalski et al., Skin mycobiota-mediated antagonism against *Staphylococcus aureus* through a modified fatty acid, Current Biology (2025), https://doi.org/10.1016/j.cub.2025.03.055

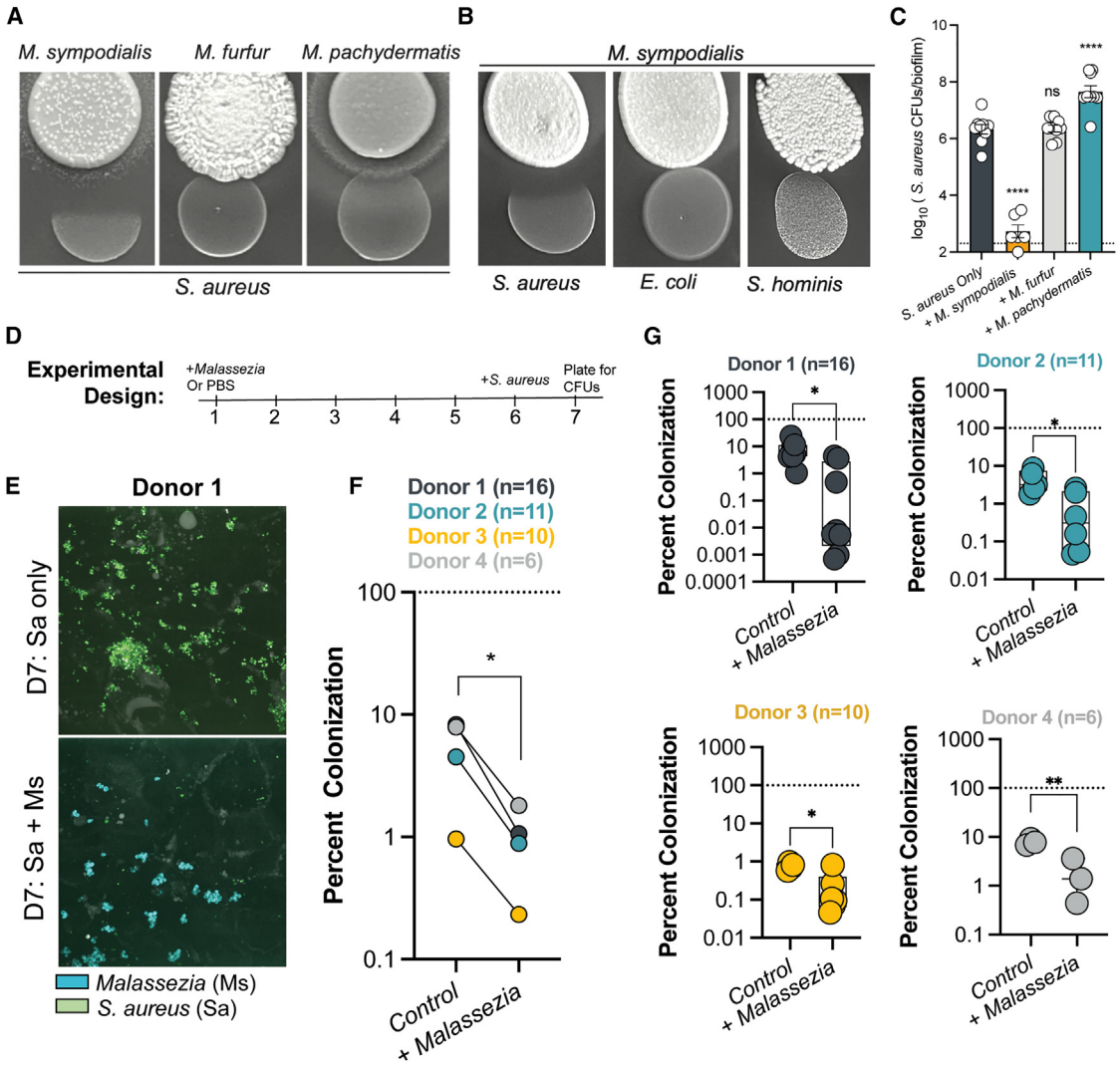

Figure 1. *Malassezia sympodialis* inhibits *S. aureus in vitro* and on human skin

(A and B) Representative images of *S. aureus* NRS193, *E. coli* Nissle, or *S. hominis* SK119 24 h growth adjacent to *M. sympodialis*, *M. furfur*, or *M. pachydermatis* grown on mDixon for 72 h.

(C) *S. aureus* NRS193 CFUs after 6 days of colony biofilm growth alone or with *M. sympodialis*, *M. furfur*, or *M. pachydermatis*. One-way ANOVA with Dunnett's multiple comparisons test. Data pooled from three separate experiments; each point represents one biofilm (n = 9 per condition). Four biofilms with *M. sympodialis* had no recovered *S. aureus* above the limit of detection (200 CFUs/mL).

(D) Experimental design for *M. sympodialis* and *S. aureus* co-colonization of human skin biopsies.

(E) Representative maximum projection images of day 7 skin surface colonized with *M. sympodialis* (cyan) and/or *S. aureus* (green).

(F) Recovered *S. aureus* CFUs per human skin biopsy from four skin donors. Each point is the average for each condition for each donor. Colors correspond to donor. Paired t test.

(G) Recovered *S. aureus* CFUs per human skin biopsies separated by individual donors; each point represents a biopsy. *$p < 0.05$, **$p < 0.01$, ***$p < 0.001$, ****$p < 0.0001$. Error bars indicate SEM. See also Figures S1A and S1B.

skin biopsies with *S. aureus* for 24 h before treating with pH-matched media or *M. sympodialis*-CFS for 24 h. Biopsies were disrupted to recover *S. aureus*, and we observed a significant reduction in *S. aureus* from biopsies treated with *M. sympodialis*-CFS compared with the control (Figure 2C). Of note, the skin colonization experiment was performed with an *S. aureus* strain expressing red fluorescent protein (RFP), which is susceptible to *M. sympodialis*-CFS (Figure S2A), but similar results are observed with *S. aureus* NRS193 (Figure S2B). Together, these data indicate that *M. sympodialis* cultured *in vitro* produces extracellular antimicrobials with bactericidal activity against *S. aureus* that can reduce colonization on human skin.

Skin commensal staphylococci have reduced susceptibility to *M. sympodialis* extracellular products

S. aureus only transiently colonizes most healthy epidermal sites, and stable colonization occurs predominantly in the anterior

Please cite this article in press as: Kowalski et al., Skin mycobiota-mediated antagonism against *Staphylococcus aureus* through a modified fatty acid, Current Biology (2025), https://doi.org/10.1016/j.cub.2025.03.055

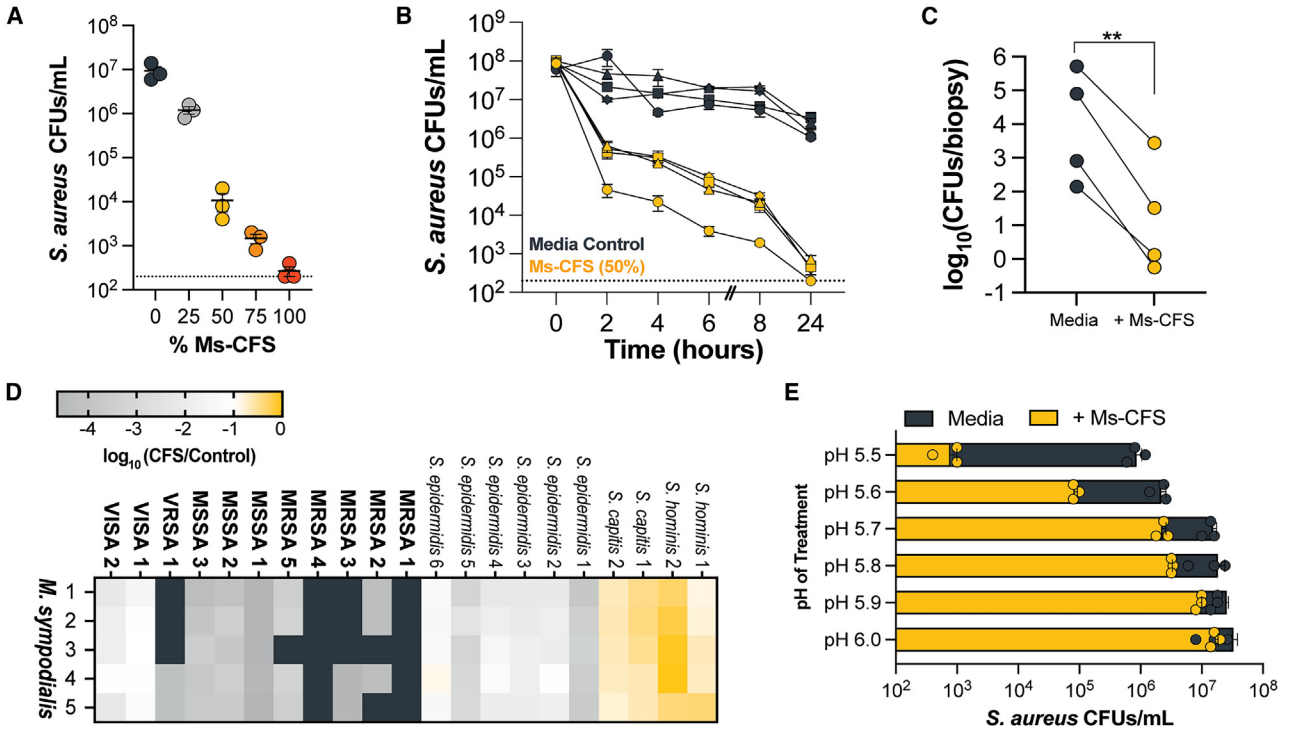

Figure 2. *M. sympodialis* produces bactericidal products with activity against *S. aureus*

(A) *S. aureus* NRS193 CFUs after treatment with CFS collected from *M. sympodialis* (Ms-CFS). Data from three experiments.

(B) *S. aureus* CFUs from four strains (2 MSSA: diamond, square; 2 MRSA: triangle, circle) over 24 h in of 50% Ms-CFS (orange) or pH-matched media control (gray).

(C) *S. aureus* CFUs (RFP-expressing strain) recovered from skin biopsies after 24 h colonization followed by 24 h treatment with Ms-CFS or pH-matched media. Each point represents the average across biopsies for a single donor. $n = 4$ donors. Paired t test.

(D) Log transformed ratio of staphylococcal CFUs from 2 h Ms-CFS treatment relative to control (media). Rows correspond to CFS from five *M. sympodialis* strains. Columns correspond to different staphylococci. Dark gray squares indicate where CFUs from the Ms-CFS treatment were below the limit of detection.

(E) *S. aureus* CFUs after 2 h MS-CFS treatment (orange) or pH-matched media (gray) from pH 5.5 to 6.0. Data from three experiments. $^{*}p < 0.05$, $^{**}p < 0.01$, $^{***}p < 0.001$, $^{****}p < 0.0001$. Error bars indicate SEM.

See also Figures S1C–S1E and S2.

nares, axillae, and groin.[3,4] In contrast, coagulase-negative staphylococci are members of the healthy skin microbiota, including *Staphylococcus epidermidis*, *Staphylococcus capitis*, and *S. hominis*.[35] As *Malassezia* are the dominant fungal colonizers of most skin sites, these yeasts likely coexist with commensal staphylococci.[19] Thus, we hypothesized that commensal staphylococci would survive exposure to *M. sympodialis*-CFS. We treated two *S. hominis* strains, two *S. capitis* strains, six *S. epidermidis* strains, and eleven *S. aureus* strains with *M. sympodialis*-CFS prepared from five *M. sympodialis* strains. Most *S. aureus* strains showed greater than 100-fold reduction in viability after 2 h *M. sympodialis*-CFS treatment (Figure 2D). Only vancomycin intermediate *S. aureus* (VISA) strains showed less than 100-fold reduction in viability. In contrast, *S, hominis* and *S. capitis* were largely unaffected by *M. sympodialis*-CFS, with less than a 10-fold reduction in viability observed. *S. epidermidis* sensitivity varied, with some strains experiencing ~10-fold reduction, whereas others phenotypically resembled *S. aureus* (Figure 2D). These data are consistent with the model that skin-resident staphylococci have strategies to coexist with *M. sympodialis*.

The antimicrobial activity of *Malassezia* extracellular products requires an acidic environment

Skin is highly acidic compared with most other body sites, and sebaceous sites in particular have a surface pH < 5.[36] Acidity contributes to the innate barrier defense of the epidermis against *S. aureus*.[6] *M. sympodialis* acidifies mDixon over 96 h, and prior experiments with *M. sympodialis*-CFS were adjusted to pH 5.5 with a pH-matched media control. As shown in Figure 2B, *S. aureus* viability gradually decreases over 24 h in mDixon media at pH 5.5. We hypothesized this was due to the acidity, as *S. aureus* grows in mDixon at pH 6 (Figure S1E). To alleviate the media toxicity, we adjusted *M. sympodialis*-CFS and pH-matched media to pH 6. Surprisingly, *M. sympodialis*-CFS toxicity was abolished at pH 6 (Figure S2C). When tested over a pH range from pH 5.5 to 6.0, 2 h *M. sympodialis*-CFS treatment only reduced *S. aureus* viability by greater than 10-fold between pH 5.5 and 5.6 (Figure 2E). Based on this result, we conclude that *M. sympodialis*-CFS toxicity requires an acidic environment like that which occurs on skin.

We suspect previous studies investigating *Malassezia*-*S. aureus* interactions did not observe antagonism due to this

Please cite this article in press as: Kowalski et al., Skin mycobiota-mediated antagonism against *Staphylococcus aureus* through a modified fatty acid, Current Biology (2025), https://doi.org/10.1016/j.cub.2025.03.055

unique pH sensitive activity.[36–40] We thus revisited *Malassezia* species unable to inhibit *S. aureus* when cultured together (Figure 1). *M. furfur* and *M. pachydermatis* do not acidify the CFS to the same extend as *M. sympodialis*, but, when adjusted to pH 5.5, the CFS from these species, as well as the two most prevalent species, *M. globosa* and *Malassezia restricta*, are able to kill *S. aureus* (Figures S2D and S2E). These data suggest that antagonism of *S. aureus* through antimicrobial extracellular products is conserved across multiple *Malassezia* species and that the activity is uniquely active within the acidic skin microenvironment.

M. sympodialis antimicrobial activity perturbs the cell membrane and is exacerbated by skin-relevant membrane stressors

Rapid killing of *S. aureus* by *M. sympodialis*-CFS appears to be independent of bacterial growth, as *S. aureus* CFUs do not increase within the 2-h exposure to the pH-matched media control (Figure 2B). Antimicrobials with rapid activity against non-growing cells often target non-biosynthetic processes, such as lipid membrane homeostasis.[41] Additionally, acidic conditions can exacerbate membrane stress.[42] Thus, we hypothesized that the *M. sympodialis*-CFS results in membrane perturbation. As membranes become permeabilized, ATP and other cytoplasmic contents leak from the cell into the extracellular milieu. We measured the ratio of extracellular ATP (eATP) to intracellular ATP (iATP) during 1 h exposure of *S. aureus* to *M. sympodialis*-CFS. As *S. aureus* killing occurred, eATP/iATP increased, consistent with membrane perturbation and cytoplasmic leakage (Figure S2F). *M. sympodialis*-CFS-treated cells also uptake the typically membrane-impermeable dye propidium iodide (PI), indicative of compromised membrane integrity (Figure S2G).

In addition to its acidity, the epidermis contains sodium chloride from sweat and free fatty acids (FFAs) from sebum that can impact bacterial membrane homeostasis.[43] We sought to determine whether these innate skin features impact *M. sympodialis*-CFS toxicity to *S. aureus*. We applied a low, nontoxic dose of *M. sympodialis*-CFS (20%) over 2 h and added subinhibitory concentrations of the FFAs lauric acid (LAU) or linoleic acid (LA). The addition of either FFA significantly enhanced killing of *S. aureus* by the *M. sympodialis*-CFS but not in the pH-matched media control (Figure S2H). Differences in FFA abundance between media types could contribute to variation in *M. sympodialis*-CFS potency. Similarly, addition of 100 mM NaCl in 20% *M. sympodialis*-CFS significantly increased the toxicity of the *M. sympodialis*-CFS treatment (Figure S2H). Together, these data suggest that *M. sympodialis* antagonism of *S. aureus* is especially potent within the skin microenvironment and that the activity is exacerbated by membrane stressors.

M. sympodialis produces an antimicrobial HP isomer

We next sought to identify the *M. sympodialis* antimicrobial effector. The activity was not impacted by boiling, denaturing, or protease treatment (Figure 3A). Thus, we hypothesized that the effector was not proteinaceous. We attempted to estimate the effector size using molecular weight cutoffs. Surprisingly, pH altered the fraction where activity eluted. At pH ~5.5, *M. sympodialis*-CFS activity was retained >10 kDa, but at pH 7, *M. sympodialis*-CFS activity eluted <10 kDa (Figure S3A). This suggested that the effector is less soluble at low pH and that acid precipitation could be applied to precipitate the effector for analysis by liquid chromatography-tandem mass spectrometry (LC-MS/MS).

Hydrochloric acid was added to media or *M. sympodialis*-CFS and the precipitate collected through centrifugation (Figure S3B). The remaining liquid fraction, now termed the acid-precipitated (AP-) fraction (AP-media or AP-CFS), was readjusted to pH 5.5 and assessed for antimicrobial activity. AP-media resembled the media control with little impact on *S. aureus* viability. AP-CFS was no longer toxic to *S. aureus*, indicating removal of the effector in the precipitate (Figure 3B). To test whether acid treatment compromised the effector, precipitates from *M. sympodialis*-CFS (CFS-P) or media (media-P) were resuspended in DMSO and spiked into the media, AP-media, or AP-CFS at 1% v/v. CFS-P, but not media-P, reduced *S. aureus* viability by at least 1,000-fold (Figure 3C). Based on these results, LC-MS/MS was performed to identify compound(s) specifically enriched in CFS-P.

We detected a peak with a higher intensity in CFS-P compared with AP-CFS, which was also present in *M. sympodialis*-CFS and absent in media controls (*m/z* 271.22, 9.5 min) (Figures S3C and S3D). This peak was hypothesized to be a HP isomer, as suggested by the LC-MS/MS dereplication tool, SIRIUS. To validate that this compound was associated with CFS-P activity, we obtained extracted ion chromatograms (EICs) for all samples at *m/z* 271.22 and identified peaks with the same mass at different retention times in inactive samples, indicating the presence of a different isomer in the media (Figure S3D). We acquired purified HPs and compared their mass fragment patterns and retention times under identical LC-MS/MS analysis conditions. The isomer detected in the media was confirmed to be 16-HP, abundant in plant cuticles and likely introduced through malt extract in the media (Figures S3E and S3G). The isomer unique to *M. sympodialis*-CFS and CFS-P conditions was identified as 10-HP, as confirmed through comparative analysis with a 10-HP standard (Figures S3F and S3H). When spiked into AP-CFS (where the effector was removed), 10-HP is antibacterial against *S. aureus* at concentrations as low as 6.25 μg/mL after 4 h (Figure 3D). In contrast, palmitic acid or 16-HP at concentrations 4× higher have negligible impacts on *S. aureus* viability (Figures 3E and 3F).

Because *S. hominis* and *S. capitis* can tolerate *M. sympodialis*-CFS (Figure 2D), we hypothesized that they would be tolerant to 10-HP. Exposure to purified 10-HP spiked into AP-CFS does not impact either species over 4 h (Figure 3G). We next sought to determine whether 10-HP could reduce *S. aureus* skin colonization similar to *M. sympodialis*-CFS. After 24 h of *S. aureus* colonization on skin, 10-HP was added for 24 h before *S. aureus* was recovered. 10-HP treatment, but not 16-HP (Figure S3I), significantly reduced *S. aureus* colonization; however, the magnitude was less than observed for *M. sympodialis*-CFS (Figure 2C) or when co-colonized with *M. sympodialis* (Figures 1F and 1G). We hypothesized additional stressors present in *M. sympodialis*-CFS or induced by *M. sympodialis* on skin exacerbate 10-HP antibacterial activity. The exacerbation of *M. sympodialis*-CFS toxicity by acidity, high salinity, and FFAs

Please cite this article in press as: Kowalski et al., Skin mycobiota-mediated antagonism against *Staphylococcus aureus* through a modified fatty acid, Current Biology (2025), https://doi.org/10.1016/j.cub.2025.03.055

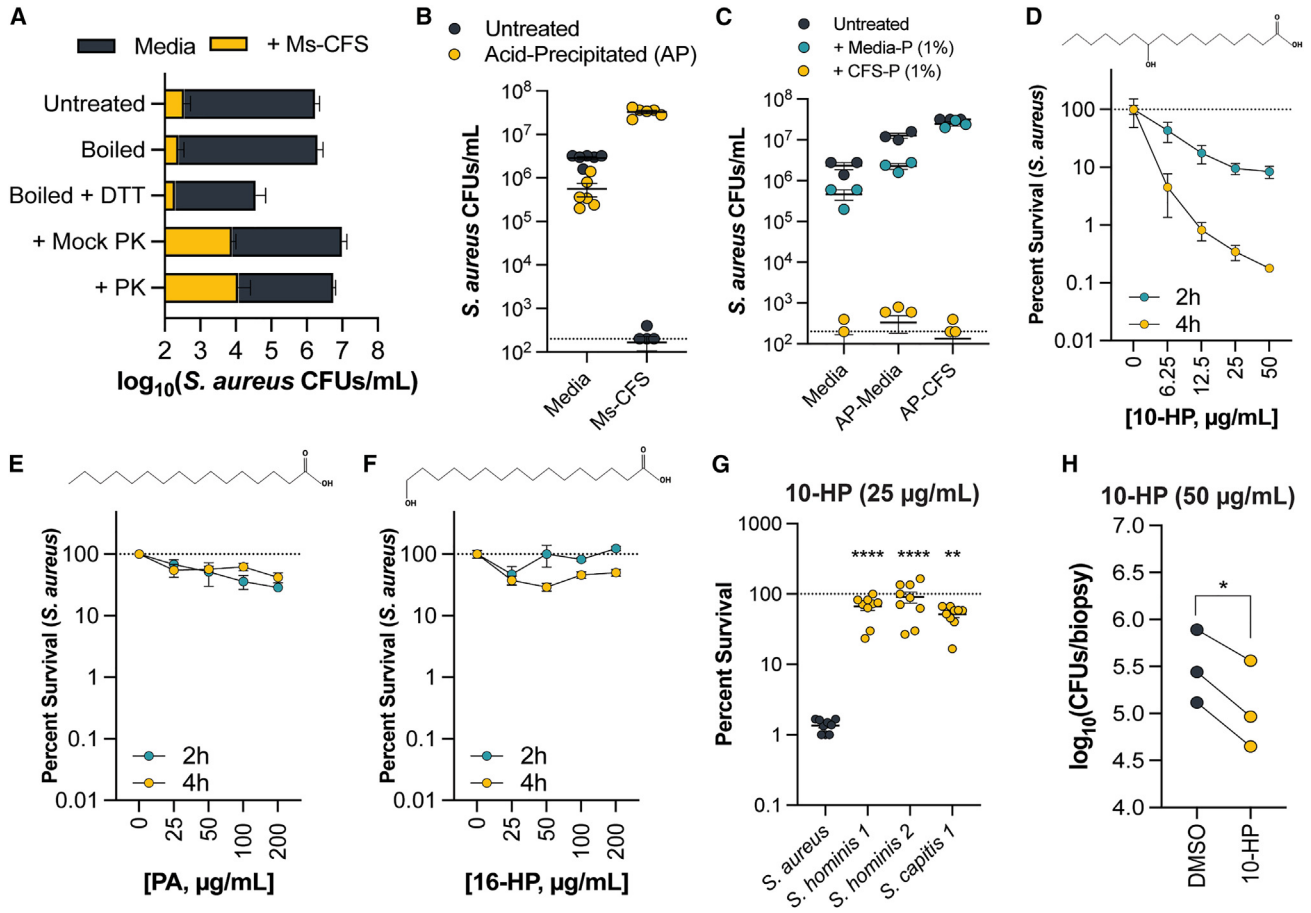

Figure 3. *M. sympodialis* produces antimicrobial 10-HP *in vitro*

(A) *S. aureus* CFUs following 2 h *M. sympodialis*-CFS (Ms-CFS) exposure or pH-matched control. PK, proteinase K.

(B) *S. aureus* CFUs following 2 h Ms-CFS exposure or pH-matched control after acid precipitation (precipitate removed) or untreated.

(C–F) (C) *S. aureus* CFUs following 2 h exposure to media, acid-precipitated media (AP-media), or AP-CFS with or without precipitate from AP-media (media-P) or AP-CFS (CFS-P). Percent survival of *S. aureus* recovered after 2 or 4 h exposure to 10-HP (D), PA (E), or 16-HP (F) relative to vehicle control in AP-CFS.

(G) *Staphylococcus* CFUs following 4 h 10-HP exposure in AP-CFS. Data from three experiments. One-way ANOVA with Dunnett's multiple comparisons test.

(H) *S. aureus* CFUs recovered from skin biopsies after 24 h 10-HP treatment. Points represent biopsy average per donor; $n = 3$ donors. Paired t test. $^{*}p < 0.05$, $^{**}p < 0.01$, $^{***}p < 0.001$, $^{****}p < 0.0001$. Error bars indicate SEM. See also Figures S3 and S4.

supports this hypothesis (Figures 2E and S2H). Indeed, treatment in tryptic soy broth (TSB), a lipid poor media, at neutral pH only reduces *S. aureus* viability with 100 µg/mL 10-HP. In contrast, *S. aureus* growth and viability are significantly reduced with 25 µg/mL 10-HP in TSB at pH 5.5 (Figures S3J and S3K). In further support of our hypothesis that 10-HP is exacerbated by additional stressors in AP-CFS, cells in AP-CFS are positive for PI staining for loss of membrane integrity in the absence of a loss of viability (Figure S2G). Positive staining then significantly increases with the addition of 10-HP.

Together, these data indicate that *M. sympodialis* produces 10-HP *in vitro* and that 10-HP has antimicrobial activity in the presence of additional stressors. Notably, *S. aureus* has been observed to generate 10-HP from palmitoleic acid (C16:1n − 7) through its oleate hydratase.[44] The authors expose *S. aureus* to 30 µM 10-HP in standard laboratory conditions without evident toxicity, and this is consistent with our observations with 25 µg/mL 10-HP (~91 µM) in TSB pH 7.

Spontaneous tolerance of *S. aureus* to *M. sympodialis* coincides with tolerance to 10-HP and a competitive advantage on *Malassezia*-colonized skin

Having identified 10-HP as the antimicrobial effector, we sought to investigate its role in colonization resistance against *S. aureus* on human skin (Figure 1). Genetic tools to characterize *M. sympodialis* gene(s) involved in 10-HP production remain limited. Therefore, we opted to use an isogenic *S. aureus* strain set with and without sensitivity to 10-HP and compete these strains on human skin in the presence and absence of *M. sympodialis*. We isolated a strain of *S. aureus* NRS193 (named EVOL-D) that evolved spontaneous tolerance to *M. sympodialis* in a 6-day mixed biofilm (Figure S4A). EVOL-D also survives *M. sympodialis*-CFS treatment (Figure S4B), suggesting toxicity is the same in mixed biofilms and *M. sympodialis*-CFS. Importantly, when challenged with 10-HP, EVOL-D survives significantly better than the ancestral strain (Figure 4A). EVOL-D colonies are small, hyperpigmented,

Please cite this article in press as: Kowalski et al., Skin mycobiota-mediated antagonism against *Staphylococcus aureus* through a modified fatty acid, Current Biology (2025), https://doi.org/10.1016/j.cub.2025.03.055

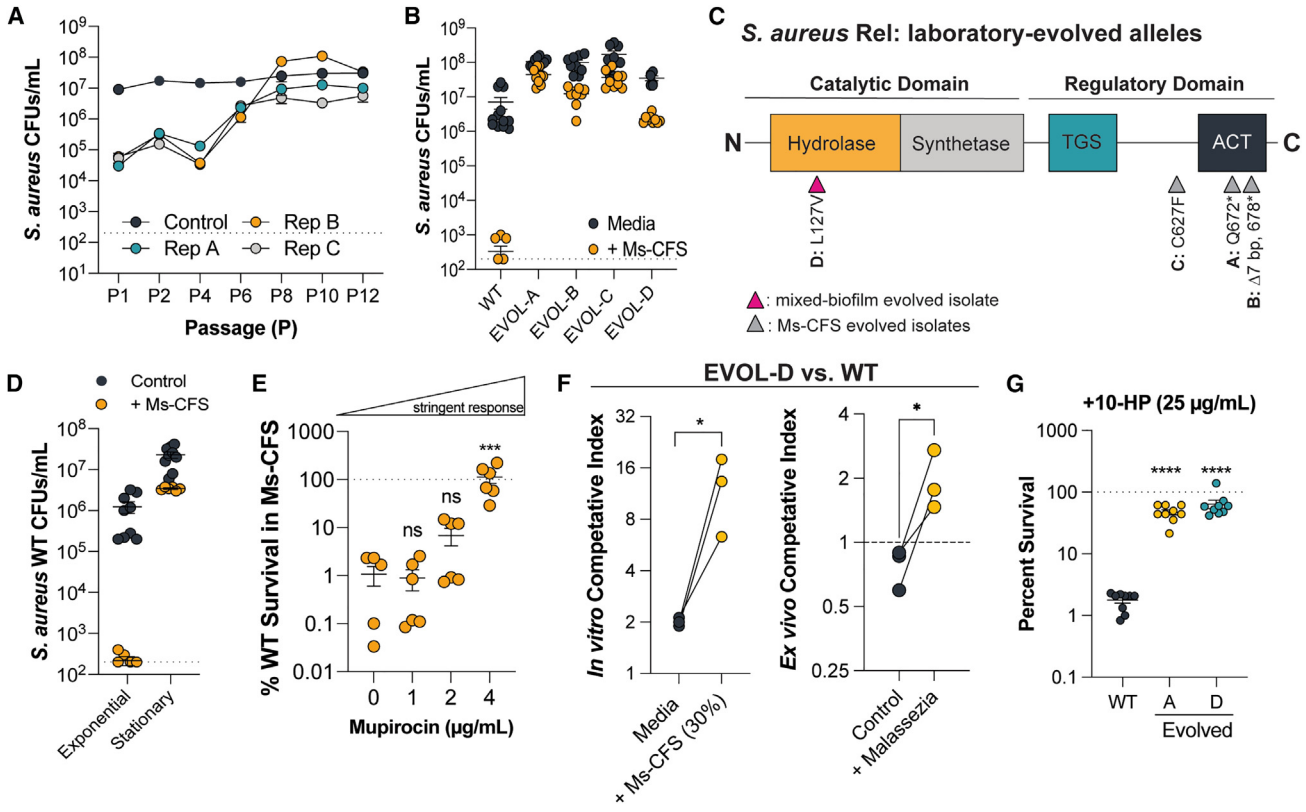

Figure 4. *S. aureus* mutations that activate the SR result in tolerance to *Malassezia* antimicrobial activity

(A) *S. aureus* percent survival following 4 h 10-HP treatment relative to control. Data from three experiments. One-way ANOVA with Dunnett's multiple comparisons test.

(B) Competitive index for EVOL-D vs. WT (1:1) *in vitro* with *M. sympodialis*-CFS (Ms-CFS) (30%) and *ex vivo* on skin biopsies with and without *M. sympodialis*. *Ex vivo* points represents biopsy average per donor. Paired t test.

(C) *S. aureus* CFUs from serial passaging in pH-matched mDixon (control) or Ms-CFS (Rep A–C).

(D) *S. aureus* CFUs from WT or evolved isolates after exposure to media or Ms-CFS. Data from three experiments.

(E) Diagram of *S. aureus* Rel with approximate locations of evolved Rel alleles.

(F) *S. aureus* CFUs following 2 h Ms-CFS treatment from exponential or stationary phase. Data from two experiments.

(G) Survival of *S. aureus* after 2 h Ms-CFS treatment in the presence or absence of mupirocin. Data from two experiments.

One-way ANOVA with Dunnett's multiple comparisons test. $^{*}p < 0.05$, $^{**}p < 0.01$, $^{***}p < 0.001$, $^{****}p < 0.0001$. Error bars indicate SEM. See also Figures S4 and S5A–S5F and Table S1.

and easily distinguishable from WT (Figure S4C). We mixed WT and EVOL-D 1:1 and treated them with a low concentration of *M. sympodialis*-CFS (30%) for 2 h. As expected, EVOL-D had a significant competitive advantage against WT in *M. sympodialis*-CFS compared with controls (Figure 4B). When the strains were competed 1:1 on human skin in the presence or absence of *M. sympodialis*, EVOL-D showed a significant competitive advantage over WT on *Malassezia*-colonized skin compared with the control (Figure 4B). These data support the hypothesis that 10-HP contributes to *Malassezia*-mediated colonization resistance on human skin.

S. aureus evolves tolerance to *M. sympodialis* antagonism through mutations in the SR regulator Rel

To dissect the mechanism of tolerance to *M. sympodialis* and 10-HP, we applied experimental evolution to select for *S. aureus* tolerance to *M. sympodialis*-CFS. Here, *S. aureus* NRS193 was exposed to *M. sympodialis*-CFS for 12 passages, where surviving cells were recovered between each passage in TSB. This was performed with three independent populations (Rep A, Rep B, and Rep C) (Figure 4C). A control population serially exposed to pH-matched media was performed in parallel. From passage 12, we isolated *M. sympodialis*-CFS tolerant colonies from each population (Rep A: EVOL-A, Rep B: EVOL-B, Rep C: EVOL-C) (Figure 4D). EVOL-A was also more tolerant to mPDB *M. sympodialis*-CFS and CFS from other *Malassezia* species (Figures S4D and S4E), suggesting that underlying toxicity is similar regardless of media type or *Malassezia* species.

We next performed genome sequencing to identify mechanisms underlying phenotypic tolerance. In each *M. sympodialis*-CFS-evolved tolerant strain, we identified mutations in the C-terminal regulatory domain of the SR regulator Rel (Figure 4E; Table S2). EVOL-D also had a Rel mutation in the N-terminal hydrolase domain (Figure 4E). Notably, isolates from the final passage of the Rep A population lacking *M. sympodialis*-CFS tolerance encoded the ancestral *rel* allele (Figure S4F). We

Please cite this article in press as: Kowalski et al., Skin mycobiota-mediated antagonism against *Staphylococcus aureus* through a modified fatty acid, Current Biology (2025), https://doi.org/10.1016/j.cub.2025.03.055

performed the same evolution experiment with a USA300 clinical isolate and again observed a mutation in *rel* associated with tolerance (Figures S4G and S4H) (Table S2). Like EVOL-D, evolved *M. sympodialis*-CFS tolerance in EVOL-A coincided with 10-HP tolerance (Figure 4A). Together, these data suggest that mutations in the SR regulator Rel contribute to *S. aureus* survival during *M. sympodialis* antagonism.

Partial activation of the SR results in *S. aureus* tolerance to *M. sympodialis* antagonism

SR is typically activated in response to starvation, where Rel interacts with stalled ribosomes, allowing for synthesis of 5′-diphosphate 3′-diphosphate (ppGpp) or 5′-triiphosphate 3′-diphosphate (pppGpp), also referred to as (p)ppGpp or alarmones.[45] In *S. aureus*, *rel* is a conditionally essential gene due to the requirement for a functional hydrolase domain that reduces the alarmone pool, which, if too high, stalls bacterial growth.[46,47] Mutations that partially activate SR have been described previously to mediate antibiotic tolerance; however, we are unaware of reports where SR facilitates tolerance to intermicrobial antagonism or antimicrobial fatty acids.[48]

Stationary phase growth or treatment with mupirocin during the exponential phase activate SR in *S. aureus*.[49–51] Prior experiments were performed with *S. aureus* from the exponential phase. To determine whether SR activation promotes *S. aureus* tolerance to *M. sympodialis*-CFS, we exposed WT stationary phase cells and exponential phase cells induced with mupirocin to *M. sympodialis*-CFS. Stationary phase cells tolerated *M. sympodialis*-CFS treatment, with only ∼10-fold reduction in viability (Figure 4F). Similarly, exponential phase cells treated with increasing levels of mupirocin were able to now tolerate *M. sympodialis*-CFS (Figure 4G), suggesting SR activation is sufficient for *M. sympodialis*-CFS tolerance.

SR activation in MRSA strains results in homogeneous resistance to β-lactams, evident by increased population growth at higher doses of β-lactams.[52] The minimum inhibitory concentration (MIC) of oxacillin for NRS193 is 2–4 μg/mL, whereas the MIC for EVOL-A and EVOL-D is 16–32 μg/mL oxacillin. Additionally, *M. sympodialis*-CFS-tolerant strains grow significantly more than WT with 4 μg/mL oxacillin (Figures S5A and S5B). These data support the hypothesis that SR is partially activated under basal conditions in EVOL-A and EVOL-D. Homogeneous resistance relies on increased MecA expression, so we deleted *mecA* in EVOL-A to assess its role in *M. sympodialis*-CFS tolerance.[53] Although loss of *mecA* reduced growth with oxacillin, *M. sympodialis*-CFS tolerance was unaffected (Figures S5C and S5D).

We next quantified pppGpp at basal state and after SR induction.[49] Under basal conditions, pppGpp was below the level of detection in all strains, but, after induction, EVOL-D showed a significant increase in pppGpp compared with WT (Figures S5E and S5F). This is consistent with another characterized *rel* allele (F128Y) that leads to SR activation and alarmone accumulation.[48] In contrast, EVOL-A, with a truncated C terminus, did not produce pppGpp at levels increased from WT after induction (Figures S5E and S5F), most likely because Rel can no longer interact with ribosomes to sense and respond to amino acid starvation. The observation that all strains had undetectable alarmone levels at basal state reflects the sensitivity of the assay and that even elevated alarmones in tolerant strains must be low enough to allow *S. aureus* growth. Based on the phenotyping data, we conclude the evolved tolerant strains have a constitutive, partial SR activation.

Laboratory-evolved *rel* alleles are necessary and sufficient for *S. aureus* tolerance to *M. sympodialis* extracellular products

To confirm that the mutated *rel* alleles are necessary and sufficient for *M. sympodialis*-CFS tolerance, we generated allele swaps. When the ancestral WT *rel* allele was replaced with the EVOL-A allele (Q672*, $WT^{Rel\text{-}A}$) or the EVOL-D allele (L127V, $WT^{Rel\text{-}D}$), the strains survived significantly better in *M. sympodialis*-CFS (Figure 5A) and displayed homogeneous β-lactam resistance (Figure S5G). Similarly, when EVOL-A and EVOL-D *rel* alleles were replaced with WT (EVOL-$A^{Rel\text{-}WT}$ and EVOL-$D^{Rel\text{-}WT}$) there was a significant reduction in *M. sympodialis*-CFS survival (Figure 5A) and a concomitant loss of homogeneous β-lactam resistance (Figure S5G). These data indicate that the evolved *rel* alleles are necessary and sufficient for survival when exposed to *M. sympodialis* products.

Rel alleles from natural *S. aureus* strains confer tolerance to *M. sympodialis* antagonism

Rel mutations have been identified in *S. aureus* clinical strains.[48,54,55] One of the first characterized natural Rel mutations, F128Y, was identified from a case of persistent bacteremia and associated with multidrug tolerance.[48] F128Y is one position away from the L127V mutation in EVOL-D (Figure 5B). We sought to determine whether natural Rel variants impacted *M. sympodialis*-CFS and 10-HP tolerance. As expected, based on similarity to EVOL-D, replacing the ancestral allele with the F128Y allele in NRS193 increased growth in oxacillin (Figure S5H), increased survival in *M. sympodialis*-CFS (Figure 5C), and reduced 10-HP sensitivity (Figure 5D). In the case of F128Y and L127V, we expect that these alleles reduce hydrolase activity, resulting in elevated (p)ppGpp.[48]

Natural Rel variants with mutations near or within the C-terminal ACT domain (Figure 5B) have also been described recently.[55] Truncation of the ACT domain may lead to SR activation by abolishing ligand binding, which modulates hydrolase activity.[56–58] We queried the NCBI Identical Protein Groups database for Rel alleles with C-terminal truncations (Table S3). We selected three truncation alleles, A567*, E657*, and Δ11 bp, which results in truncation at position 658 (Δ11 bp, 658*) (Figure 5B). We replaced the NRS193 WT *rel* allele with these variants and all three increased survival in oxacillin, *M. sympodialis*-CFS, and 10-HP (Figures 5C, 5D, and S5H). The fact that these natural Rel variants lead to *S. aureus* tolerance to *M. sympodialis* antagonism suggests that SR activation could concomitantly result in *S. aureus* overcoming microbiota-mediated colonization resistance or that microbiota antagonism can select for mutations conferring SR activation, with consequences for antibiotic treatment.[59]

Laboratory-evolved *rel* alleles increase *S. aureus* tolerance to clinical antibiotics

We sought to determine whether the evolved Rel alleles, Rel-A (Q672*) and Rel-D (L127V), impacted antibiotic tolerance similar

Please cite this article in press as: Kowalski et al., Skin mycobiota-mediated antagonism against *Staphylococcus aureus* through a modified fatty acid, Current Biology (2025), https://doi.org/10.1016/j.cub.2025.03.055

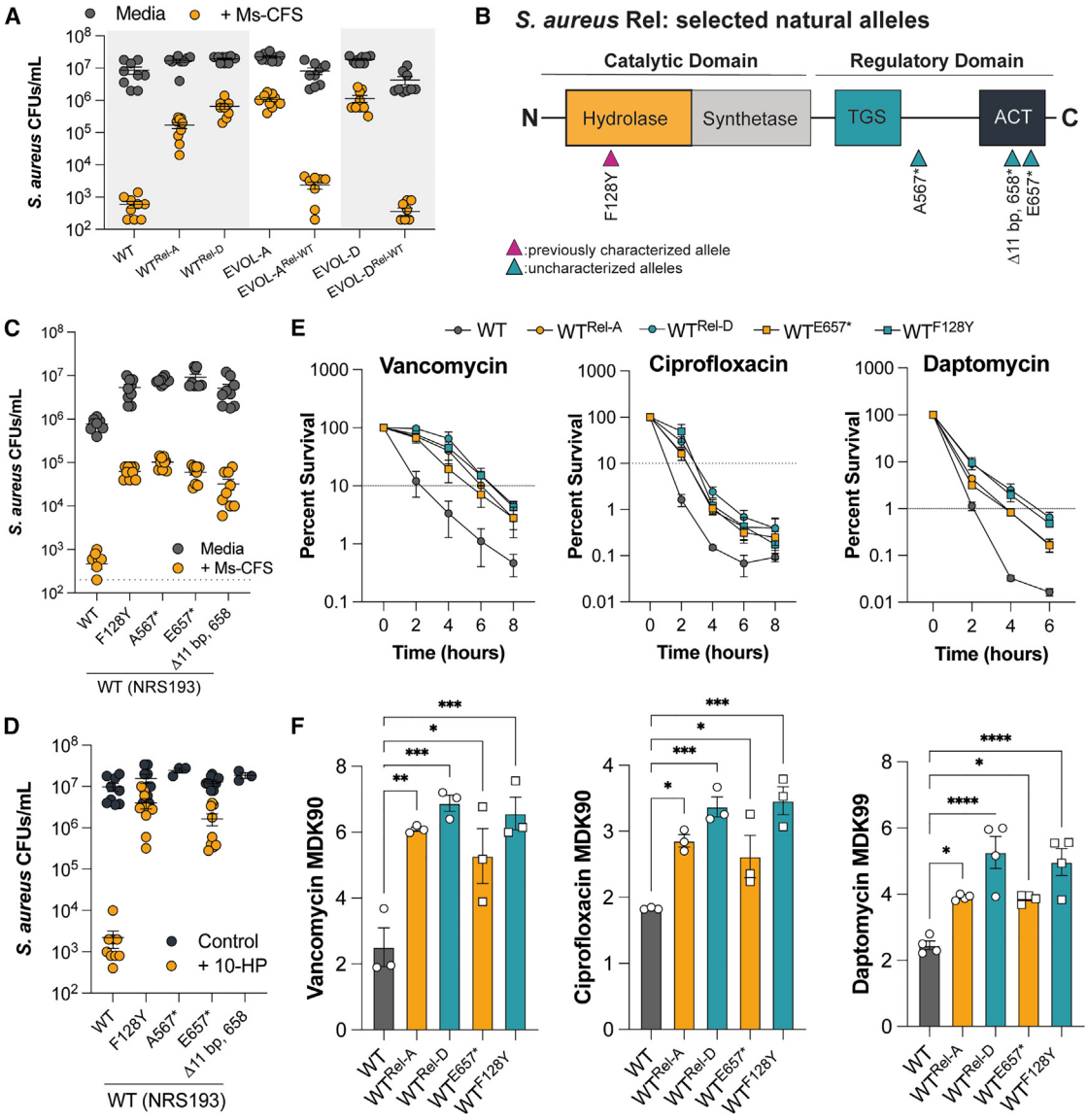

Figure 5. Natural Rel variants that activate the SR confer tolerance to *Malassezia*, 10-HP, and clinical antibiotics

(A) *S. aureus* CFUs following 2 h *M. sympodialis*-CFS (Ms-CFS) treatment (orange) or pH-matched media control (gray). Rel-WT: NRS193 allele, Rel-A: EVOL-A Q672* allele, and Rel-D: EVOL-D L127V allele. Data from three experiments.

(B) Diagram of *S. aureus* Rel with natural alleles.

(C) *S. aureus* CFUs following 2 h Ms-CFS treatment (orange) or exposure to pH-matched media controls (gray). Alleles correspond to natural Rel alleles in (B).

(D) *S. aureus* CFUs following 4 h 10-HP treatment (orange) or vehicle control (gray). Data pooled from three experiments.

(E) Time-kill assays for *S. aureus* strains exposed to vancomycin (1 μg/mL), ciprofloxacin (0.5 μg/mL), or daptomycin (100 μg/mL). Dashed lines indicate the percent survival at which MDK was calculated. Data represent the mean from three or four experiments.

(F) MDK values from curves in (E).

One-way ANOVA with Dunnett's multiple comparisons test. *$p < 0.05$, **$p < 0.01$, ***$p < 0.001$, ****$p < 0.0001$. Error bars indicate SEM. See also Figures S5G and S5H and Table S2.

to F128Y.[48] We also included the natural variant E657*, as C-terminal Rel mutations have an unclear role in multidrug tolerance. We calculated the minimum duration of killing (MDK), the gold standard method for quantifying antibiotic tolerance.[60,61] As previously reported, F128Y is sufficient to significantly increase tolerance to vancomycin (MDK_{90}), ciprofloxacin (MDK_{90}), and daptomycin (MDK_{99}) (Figures 5E and 5F).[48,61] Our laboratory-evolved hydrolase allele, Rel-D/L127V, similarly increased tolerance to each antibiotic (Figures 5E and 5F). The C-terminal alleles also significantly increased tolerance to all three antibiotics, and although the magnitude of tolerance was similar between them, the C-terminal truncations appear to be marginally less tolerant than the N-terminal hydrolase alleles (Figures 5E and 5F). These data demonstrate that truncations at the C terminus of *S. aureus* Rel, as small as 57 amino acids (Q672*), are sufficient for multidrug tolerance. Additionally, our findings extend

Please cite this article in press as: Kowalski et al., Skin mycobiota-mediated antagonism against *Staphylococcus aureus* through a modified fatty acid, Current Biology (2025), https://doi.org/10.1016/j.cub.2025.03.055

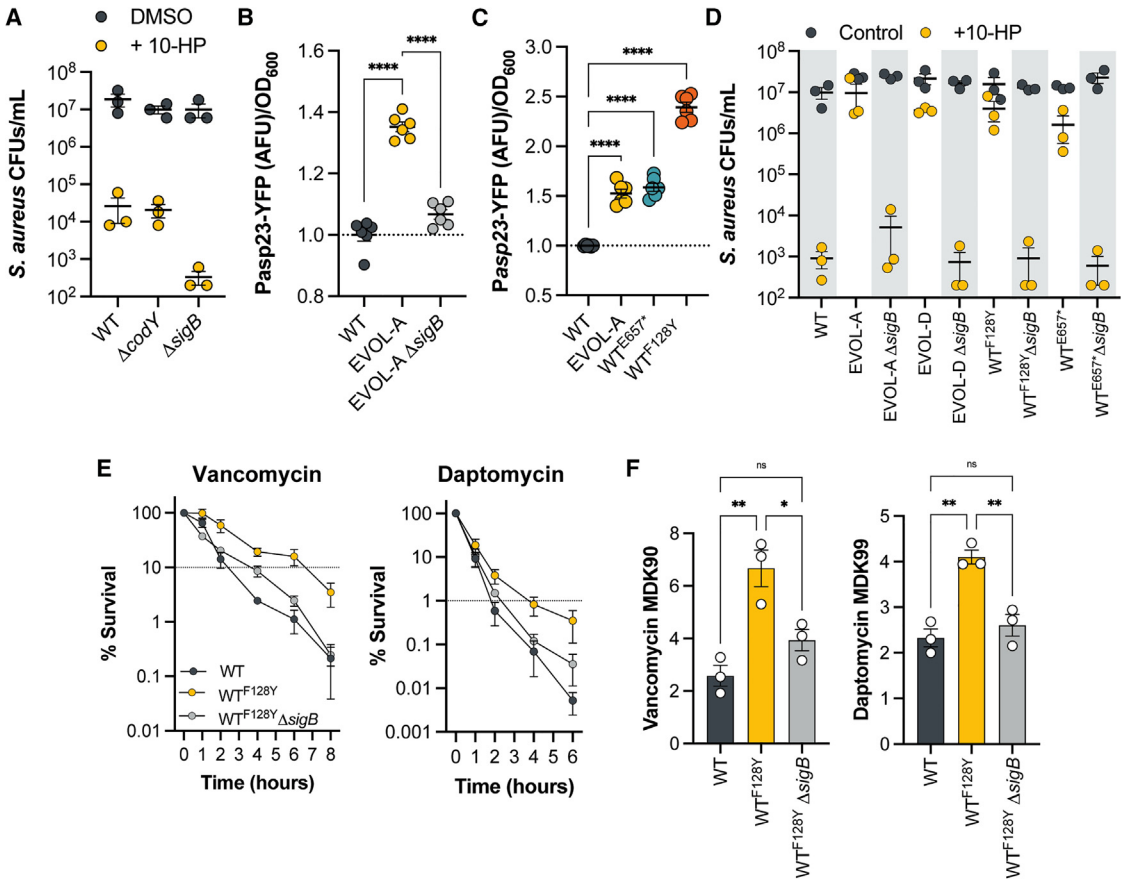

Figure 6. Increased SigB activity contributes to 10-HP and antibiotic tolerance in strains with partial SR activation

(A) *S. aureus* CFUs following 4 h 10-HP treatment or vehicle control for WT, Δ*codY*, or Δ*sigB*. Data from three experiments.

(B–C) Activity of SigB transcriptional reporter (Pasp23-YFP). Data from six experiments.

(D) *S. aureus* CFUs following 4 h 10-HP treatment or vehicle control. Data from three experiments.

(E) Time-kill assays for *S. aureus* exposed to vancomycin (1 μg/mL) or daptomycin (100 μg/mL). Dashed lines indicate percent survival where MDK was calculated. Data represent mean from three experiments.

(F) MDK values extrapolated from curves in (E).

One-way ANOVA with Dunnett's multiple comparisons test. $*p < 0.05$, $**p < 0.01$, $***p < 0.001$, $****p < 0.0001$. All error bars indicate SEM. See also Figure S6.

this tolerance from clinical antibiotics to include microbiota-derived antimicrobials.

Activation of the alternative sigma factor SigB is necessary for 10-HP and antibiotic tolerance in partially stringent strains

SR-induced multidrug tolerance was previously suggested to result from extended lag phase, a mechanism that underlies antibiotic tolerance across diverse bacteria.[60] Rel-A and Rel-D marginally reduce the *S. aureus* growth rate compared with WT in TSB during the first 4 h of growth (Figure S6A). Yet, *M. sympodialis*-CFS killing occurs rapidly without measurable *S. aureus* growth. Thus, we sought to determine what factors downstream of SR activation contribute to *S. aureus* tolerance to 10-HP and clinical antibiotics. A hallmark of SR in *S. aureus* is de-repression of the transcriptional repressor CodY,[62] but deletion of *codY* in the WT strain does not impact *M. sympodialis*-CFS (Figure S6B) or 10-HP sensitivity (Figure 6A). SR activation of alternative sigma factors is characteristic of Gram-negative bacteria, but it remains unclear how SR in Gram-positive bacteria impacts alternative sigma factors (e.g., SigB).[46] In *S. aureus*, SigB regulates production of the pigment staphyloxanthin, but although the evolved strains are hyperpigmented, the pigment itself is not necessary for *M. sympodialis*-CFS or 10-HP tolerance (Figures S6C–S6E).[63] We hypothesized that hyperpigmentation indicates elevated SigB activity and that this activity contributes to the tolerant state. In support of this, loss of *sigB* in the WT strain increases 10-HP sensitivity (Figure 6A).

We generated a transcriptional reporter for SigB activity using the *asp23* promoter.[63] In EVOL-A, at basal state, SigB activity is significantly increased compared with WT and EVOL-A lacking *sigB* (Figure 6B). Similarly, SigB activity is significantly increased in strains with natural Rel variants (WT^{E657*} and WT^{F128Y}) (Figure 6C). To determine whether increased SigB activity contributes to 10-HP and *M. sympodialis*-CFS tolerance, we generated *sigB* deletions in each Rel mutant background. When challenged with 10-HP (Figure 6D) or *M. sympodialis*-CFS (Figure S6F),

Please cite this article in press as: Kowalski et al., Skin mycobiota-mediated antagonism against *Staphylococcus aureus* through a modified fatty acid, Current Biology (2025), https://doi.org/10.1016/j.cub.2025.03.055

strains lacking *sigB* were resensitized and resembled WT. Similarly, in WT^{F128Y}, *sigB* is necessary for the enhanced tolerance to vancomycin and daptomycin (Figures 6D and 6E) but not ciprofloxacin (Figures S6G and S6H). SigB activity has previously been linked to antibiotic tolerance, and our data now highlight its important contribution to tolerance during partial SR activation.[64] Together, these results demonstrate the ability of skin-resident fungi to promote colonization resistance against *S. aureus*, as well as genetic mechanisms by which *S. aureus* adapts in the face of fungal antagonism.

DISCUSSION

Recent studies reveal that host-resident fungi, despite their relatively low abundance, have major impacts on host health.[65] But although several studies have identified mycobiota impacts on bacterial communities or dysbiosis in animals,[66,67] few studies report a role for fungi in colonization resistance.[25,68] This is despite examples in other systems, such as the cheese microbiota, where fungi have been observed to impact bacteria growth, survival, and antimicrobial susceptibility.[69,70]

Human skin hosts a unique mycobiota dominated by *Malassezia*.[20] Although *Malassezia* have been associated with several skin diseases, such as pityriasis versicolor and seborrheic dermatitis,[71] they typically colonize skin without inducing disease. This has led many to hypothesize *Malassezia* have a mutualistic relationship with the host, where these lipid-dependent yeasts thrive within the lipid-rich niche and benefit the host by inducing AMPs.[72,73] In addition to host-fungal interactions, observations support an important role for *Malassezia* interactions with other microbes. For example, in atopic dermatitis, an inflammatory disease associated with *S. aureus* skin colonization, non-*Malassezia* fungal diversity is reportedly increased relative to healthy controls.[74] Additionally, *M. globosa* secretes a protease capable of degrading *S. aureus* biofilms.[25] Our results identify a beneficial role for *Malassezia* on human skin, where *M. sympodialis* colonization significantly reduces the ability of *S. aureus* to colonize the human epidermis (Figure 1). Given the prevalence of *Malassezia* within the mammalian skin microbiota, we are likely just scratching the surface of its roles in shaping microbial interactions and colonization resistance in this niche.

As *Malassezia* lack the ability to generate fatty acids *de novo*, the production of 10-HP must require transformation of exogenous lipids. Thus, 10-HP production is likely dependent on the lipid environment and may differ between *in vitro* media and skin microenvironments. It is noteworthy that the generation of extracellular hydroxy fatty acids has been reported previously for *M. furfur* (then *Pityrosporum ovale*), where 9-HP and 9-hydroxy stearic acid are produced from stearic acid.[75] Like 10-HP, we found that 9-HP has antimicrobial activity that is pH dependent (Figures S3L and S3M). Future work will focus on characterizing lipid precursors and yeast genes necessary for 10-HP production.

Transformation of host metabolites, such as lipids, into mediators of intermicrobial antagonism, such as 10-HP, is consistent with colonization resistance through niche modification.[76] To date, most colonization resistance mechanisms described on skin are examples of active antagonism through the production of proteases, AMPs, or antibiotics.[9,25,76] FFAs on skin result from lipolysis by the microbiota, and these can impact microbial colonization and skin barrier integrity.[77] We propose that *Malassezia* mediate colonization resistance through chemical modification of these FFAs, introducing a new layer to this model that likely has implications for other skin residents. Analogous niche modification mechanisms are well documented at other body sites with impacts on microbiota and host cell functions. For example, the intestinal microbiota modifies host bile acids, generating diverse, chemically distinct compounds that contribute to colonization resistance, promote host health, and drive disease.[78] How host state, skin microenvironment, and microbiota composition impact the transformation of skin lipids into bioactive compounds, such as hydroxy fatty acids, and the impacts of these compounds on overall health are areas of future research.

The pH-dependent activity of 10-HP, and 9-HP, might contribute to the observation that *S. aureus* and *Malassezia* can co-colonize the anterior nares and the skin of atopic dermatitis patients, where the pH is less acidic than other, healthy epidermal regions.[36,74,79,80] The contribution of pH to 10-HP toxicity remains unclear, but possible explanations are that acidity induces membrane stress or facilitates interaction of 10-HP with the membrane. The pH requirement likely explains why 10-HP has not been reported as antimicrobial and why *S. aureus* can produce 10-HP itself through oleate hydratase activity in the presence of palmitoleic acid.[44] Notably, palmitoleic acid is more toxic to *S. aureus* at low pH.[81] It is tempting to speculate that this is due to oleate hydratase detoxification generating 10-HP, which is itself toxic in these conditions. The conditional toxicity of 10-HP builds upon a growing literature of antimicrobials with limited activity in standard laboratory conditions.[82–84]

The observation that skin residents *S. hominis* and *S. capitis* are not sensitive to *M. sympodialis* or 10-HP presents an opportunity to investigate the antimicrobial mechanism. The SR is highly conserved, and Rel sequences of *S. aureus*, *S. capitis*, *and S. hominis* do not reveal obvious differences that would impact activity (e.g., truncations). As tolerance to *M. sympodialis*-CFS and 10-HP in our evolved strains depends on SigB, it is likely that other mechanisms downstream of Rel/SigB differ between these species. One area of interest is the fates of extracellular fatty acids. Recently, a β-oxidation pathway for fatty acid catabolism was described in *S. aureus* with a preference for palmitic acid.[85] BLAST analyses reveal that homologs of these genes (*fadXDEBA*) are likely absent from many other staphylococci, including *S. hominis* and *S. capitis*. Exogenous fatty acids can also be incorporated into phospholipids through the action of fatty acid kinase (FakA).[86] Although FakA is conserved across staphylococci, induction of Rel synthetase activity in *S. aureus* was previously shown to significantly reduce mRNA expression of *fakA* and increase *fadX* expression.[46] This suggests that the fates of extracellular fatty acids differ between staphylococci and during SR, and this may directly impact 10-HP sensitivity.

Antibiotic tolerance describes the ability of a microorganism to survive during transient exposure to a high dose of an antibiotic.[61] Transient, non-heritable antibiotic tolerance in *S. aureus* is known to be induced by several host-relevant conditions in the absence of clinical antibiotics, including human serum,[87] the

macrophage phagolysosome,[88] and growth as a biofilm.[89] Additionally, co-culture of *S. aureus* with *C. albicans* in a dual species biofilm was observed to significantly increase *S. aureus* multidrug tolerance compared with *S. aureus* mono-species biofilms.[90,91] Inducers of heritable antibiotic tolerance in *S. aureus* are less well characterized, and it remains an open question whether, and to what degree, antagonism by other microbes selects for heritable antibiotic tolerance in the absence of antibiotics. A previous study observed that bacteriocin-producing subpopulations of *S. aureus* could select for vancomycin tolerance in bacteriocin non-producers.[92] Our *in vitro* studies build upon this literature to support the hypothesis that intermicrobial antagonism has the potential to select for stable, heritable antibiotic tolerance in bacterial pathogens such as *S. aureus*.

Although additional studies are necessary to determine how *Malassezia* shapes *S. aureus* adaptation on a host, our results suggest that natural variation, evident in *S. aureus* strains and genomic data, is sufficient for tolerance to a broad range of antimicrobials. This poses the question of how broad tolerance mechanisms could evolve from intermicrobial antagonism, with consequences for antibiotic treatment. Additionally, how *Malassezia* shapes the skin microbiota remains an open question, but the observation that *S. hominis* and *S. capitis* can tolerate growth with *M. sympodialis* and 10-HP suggests that mechanisms of tolerance exist that allow these organisms to co-colonize. Collectively our findings support a model whereby the skin-resident yeast *M. sympodialis* transforms environmental lipids into antimicrobial hydroxy fatty acids, such as 10-HP, that contribute to colonization resistance against *S. aureus* and simultaneously select for broad antibiotic tolerance.

RESOURCE AVAILABILITY

Lead contact

Requests for further information and resources should be directed to and will be fulfilled by the lead contact, Matthew Barber (mfbarber@uoregon.edu).

Materials availability

All unique reagents generated in this study are available from the lead contact without restriction.

Data and code availability

- Sequencing data have been deposited at NCBI as BioProject: PRJNA1107622 and are publicly available as of the date of publication.
- This paper does not report original code.
- Any additional information required to reanalyze the data reported in this paper is available from the lead contact upon request.

ACKNOWLEDGMENTS

We thank Dr. Joe Heitman for providing the *Malassezia* strains and Dr. Karen Guillemin for the *E. coli* Nissle strain. We also thank Dr. Kristin Kohler for critical feedback on the manuscript. This work was carried out with the support of the University of Oregon GC3F core facilities. Support for this work in the form of funding was received by C.H.K. (L'Oréal USA for Women in Science Fellowship and Helen Hay Whitney Foundation Fellowship), T.J.S. (National Institutes of Health grants 1P01GM125576, F32DK124033, and K99DK137017), M.F.B. (National Institutes of Health grants R35GM133652 and R21AI173839), R.M.C. (Sir Henry Dale Fellowship jointly funded by the Wellcome Trust and the Royal Society, 104110/Z/14/A, and a Lister Institute Research Prize Fellowship 2018), L.K. (National Institutes of Health grant U19 AI142720), and U.T.N. (National Institutes of Health for the Biotechnology Training Program, 5T32GM135066, and National Science Foundation Graduate Research Fellowship Program).

AUTHOR CONTRIBUTIONS

Conceptualization: C.H.K. and M.F.B.; methodology: C.H.K., M.F.B., L.K., and U.T.N.; investigation: C.H.K., S.L., T.J.S., U.T.N., W.S.S., and R.M.C.; writing – original draft: C.H.K. and M.F.B.; writing – reviewing & editing: U.T.N., S.L., T.J.S., R.M.C., and L.K.; and funding acquisition: C.H.K., M.F.B., L.K., and R.M.C.

DECLARATION OF INTERESTS

M.F.B. and C.H.K. are inventors on a US patent (US-11820799-B2) related to the use of *Malassezia* for treatment of bacterial infections.

STAR★METHODS

Detailed methods are provided in the online version of this paper and include the following:

- KEY RESOURCES TABLE
- EXPERIMENTAL MODEL AND STUDY PARTICIPANT DETAILS
- METHOD DETAILS
  - Bacterial and yeast culture conditions
  - Adjacent colony assay and mixed biofilms
  - Co-colonization of human skin biopsies
  - *S. aureus* competition on human skin biopsies
  - CFS preparation and treatment
  - Treatment of human skin biopsies
  - Processing of cell-free supernatant
  - Identification of antimicrobial effector
  - ATP measurements
  - Propidium iodide staining
  - Serial passaging experimental evolution
  - *S. aureus* genomic DNA preparation
  - Whole genome sequencing and variant calling
  - Mupirocin treatment
  - Bacterial growth curves
  - Genetic manipulation of *S. aureus*
  - Identification of natural Rel alleles
  - MIC and time-kill assays
  - Quantification of pppGpp
- QUANTIFICATION AND STATISTICAL ANALYSIS

SUPPLEMENTAL INFORMATION

Supplemental information can be found online at https://doi.org/10.1016/j.cub.2025.03.055.

Received: May 7, 2024
Revised: February 17, 2025
Accepted: March 21, 2025
Published: April 14, 2025

REFERENCES

1. Kaye, K.S., Petty, L.A., Shorr, A.F., and Zilberberg, M.D. (2019). Current Epidemiology, Etiology, and Burden of Acute Skin Infections in the United States. Clin. Infect. Dis. *68*, S193–S199. https://doi.org/10.1093/cid/ciz002.
2. GBD 2019 Antimicrobial Resistance Collaborators (2022). Global mortality associated with 33 bacterial pathogens in 2019: a systematic analysis for the Global Burden of Disease Study 2019. Lancet *400*, 2221–2248. https://doi.org/10.1016/S0140-6736(22)02185-7.

3. Rohr, U., Wilhelm, M., Muhr, G., and Gatermann, S. (2004). Qualitative and (semi)quantitative characterization of nasal and skin methicillin-resistant Staphylococcus aureus carriage of hospitalized patients. Int. J. Hyg. Environ. Health *207*, 51–55. https://doi.org/10.1078/1438-4639-00266.

4. Sakr, A., Brégeon, F., Mège, J.L., Rolain, J.M., and Blin, O. (2018). Staphylococcus aureus Nasal Colonization: An Update on Mechanisms, Epidemiology, Risk Factors, and Subsequent Infections. Front. Microbiol. *9*, 2419. https://doi.org/10.3389/fmicb.2018.02419.

5. Fischer, C.L., Blanchette, D.R., Brogden, K.A., Dawson, D.V., Drake, D.R., Hill, J.R., and Wertz, P.W. (2014). The roles of cutaneous lipids in host defense. Biochim. Biophys. Acta *1841*, 319–322. https://doi.org/10.1016/j.bbalip.2013.08.012.

6. Costa, F.G., and Horswill, A.R. (2022). Overcoming pH defenses on the skin to establish infections. PLOS Pathog. *18*, e1010512. https://doi.org/10.1371/journal.ppat.1010512.

7. Schauber, J., and Gallo, R.L. (2008). Antimicrobial peptides and the skin immune defense system. J. Allergy Clin. Immunol. *122*, 261–266. https://doi.org/10.1016/j.jaci.2008.03.027.

8. Flowers, L., and Grice, E.A. (2020). The Skin Microbiota: Balancing Risk and Reward. Cell Host Microbe *28*, 190–200. https://doi.org/10.1016/j.chom.2020.06.017.

9. Zipperer, A., Konnerth, M.C., Laux, C., Berscheid, A., Janek, D., Weidenmaier, C., Burian, M., Schilling, N.A., Slavetinsky, C., Marschal, M., et al. (2016). Human commensals producing a novel antibiotic impair pathogen colonization. Nature *535*, 511–516. https://doi.org/10.1038/nature18634.

10. Claesen, J., Spagnolo, J.B., Ramos, S.F., Kurita, K.L., Byrd, A.L., Aksenov, A.A., Melnik, A.V., Wong, W.R., Wang, S., Hernandez, R.D., et al. (2020). A Cutibacterium acnes antibiotic modulates human skin microbiota composition in hair follicles. Sci. Transl. Med. *12*, eaay5445. https://doi.org/10.1126/scitranslmed.aay5445.

11. Iwase, T., Uehara, Y., Shinji, H., Tajima, A., Seo, H., Takada, K., Agata, T., and Mizunoe, Y. (2010). Staphylococcus epidermidis Esp inhibits Staphylococcus aureus biofilm formation and nasal colonization. Nature *465*, 346–349. https://doi.org/10.1038/nature09074.

12. Rademacher, F., Bartels, J., Gläser, R., Rodewald, M., Schubert, S., Drücke, D., Rohde, H., and Harder, J. (2022). Staphylococcus epidermidis-Derived Protease Esp Mediates Proteolytic Activation of Pro−IL-1β in Human Keratinocytes. J. Invest. Dermatol. *142*, 2756–2765.e8. https://doi.org/10.1016/j.jid.2022.04.010.

13. Chin, D., Goncheva, M.I., Flannagan, R.S., Deecker, S.R., Guariglia-Oropeza, V., Ensminger, A.W., and Heinrichs, D.E. (2021). Coagulase-negative staphylococci release a purine analog that inhibits Staphylococcus aureus virulence. Nat. Commun. *12*, 1887. https://doi.org/10.1038/s41467-021-22175-3.

14. Severn, M.M., Williams, M.R., Shahbandi, A., Bunch, Z.L., Lyon, L.M., Nguyen, A., Zaramela, L.S., Todd, D.A., Zengler, K., Cech, N.B., et al. (2022). The Ubiquitous Human Skin Commensal Staphylococcus hominis Protects against Opportunistic Pathogens. mBio *13*, e0093022. https://doi.org/10.1128/mbio.00930-22.

15. Nakatsuji, T., Hata, T.R., Tong, Y., Cheng, J.Y., Shafiq, F., Butcher, A.M., Salem, S.S., Brinton, S.L., Rudman Spergel, A.K., Johnson, K., et al. (2021). Development of a human skin commensal microbe for bacteriotherapy of atopic dermatitis and use in a phase 1 randomized clinical trial. Nat. Med. *27*, 700–709. https://doi.org/10.1038/s41591-021-01256-2.

16. Talebi Bezmin Abadi, A., Rizvanov, A.A., Haertlé, T., and Blatt, N.L. (2019). World Health Organization Report: Current Crisis of Antibiotic Resistance. BioNanoScience *9*, 778–788. https://doi.org/10.1007/s12668-019-00658-4.

17. Oh, J., Byrd, A.L., Deming, C., Conlan, S., NISC Comparative Sequencing Program, Kong, H.H., and Segre, J.A. (2014). Biogeography and individuality shape function in the human skin metagenome. Nature *514*, 59–64. https://doi.org/10.1038/nature13786.

18. Qin, J., Li, R., Raes, J., Arumugam, M., Burgdorf, K.S., Manichanh, C., Nielsen, T., Pons, N., Levenez, F., Yamada, T., et al. (2010). A human gut microbial gene catalogue established by metagenomic sequencing. Nature *464*, 59–65. https://doi.org/10.1038/nature08821.

19. Byrd, A.L., Belkaid, Y., and Segre, J.A. (2018). The human skin microbiome. Nat. Rev. Microbiol. *16*, 143–155. https://doi.org/10.1038/nrmicro.2017.157.

20. Findley, K., Oh, J., Yang, J., Conlan, S., Deming, C., Meyer, J.A., Schoenfeld, D., Nomicos, E., Park, M., et al.; NIH Intramural Sequencing Center Comparative Sequencing Program (2013). Topographic diversity of fungal and bacterial communities in human skin. Nature *498*, 367–370. https://doi.org/10.1038/nature12171.

21. Wu, G., Zhao, H., Li, C., Rajapakse, M.P., Wong, W.C., Xu, J., Saunders, C.W., Reeder, N.L., Reilman, R.A., Scheynius, A., et al. (2015). Genus-Wide Comparative Genomics of Malassezia Delineates Its Phylogeny, Physiology, and Niche Adaptation on Human Skin. PLoS Genet. *11*, e1005614. https://doi.org/10.1371/journal.pgen.1005614.

22. Moran, N.A., and Plague, G.R. (2004). Genomic changes following host restriction in bacteria. Curr. Opin. Genet. Dev. *14*, 627–633. https://doi.org/10.1016/j.gde.2004.09.003.

23. Ianiri, G., Coelho, M.A., Ruchti, F., Sparber, F., McMahon, T.J., Fu, C., Bolejack, M., Donovan, O., Smutney, H., Myler, P., et al. (2020). HGT in the human and skin commensal Malassezia: A bacterially derived flavohemoglobin is required for NO resistance and host interaction. Proc. Natl. Acad. Sci. USA *117*, 15884–15894. https://doi.org/10.1073/pnas.2003473117.

24. Porro, M.N., Passi, S., Caprill, F., Nazzaro, P., and Morpurgo, G. (1976). Growth requirements and lipid metabolism of Pityrosporum orbiculare. J. Invest. Dermatol. *66*, 178–182. https://doi.org/10.1111/1523-1747.ep12481919.

25. Li, H., Goh, B.N., Teh, W.K., Jiang, Z., Goh, J.P.Z., Goh, A., Wu, G., Hoon, S.S., Raida, M., Camattari, A., et al. (2018). Skin Commensal Malassezia globosa Secreted Protease Attenuates Staphylococcus aureus Biofilm Formation. J. Invest. Dermatol. *138*, 1137–1145. https://doi.org/10.1016/j.jid.2017.11.034.

26. Huang, X., Welsh, R.M., Deming, C., Proctor, D.M., Thomas, P.J., Gussin, G.M., Huang, S.S., Kong, H.H., Bentz, M.L., et al.; NISC Comparative Sequencing Program (2021). Skin Metagenomic Sequence Analysis of Early Candida auris Outbreaks in U.S. Nursing Homes. mSphere *6*, e0028721. https://doi.org/10.1128/mSphere.00287-21.

27. Proctor, D.M., Dangana, T., Sexton, D.J., Fukuda, C., Yelin, R.D., Stanley, M., Bell, P.B., Baskaran, S., Deming, C., Chen, Q., et al. (2021). Integrated genomic, epidemiologic investigation of Candida auris skin colonization in a skilled nursing facility. Nat. Med. *27*, 1401–1409. https://doi.org/10.1038/s41591-021-01383-w.

28. Mohammad, H., Abutaleb, N.S., Dieterly, A.M., Lyle, L.T., and Seleem, M.N. (2021). Evaluation of ebselen in resolving a methicillin-resistant Staphylococcus aureus infection of pressure ulcers in obese and diabetic mice. PLoS One *16*, e0247508. https://doi.org/10.1371/journal.pone.0247508.

29. Bond, R., and Anthony, R.M. (1995). Characterization of markedly lipid-dependent Malassezia pachydermatis isolates from healthy dogs. J. Appl. Bacteriol. *78*, 537–542. https://doi.org/10.1111/j.1365-2672.1995.tb03096.x.

30. Ianiri, G., Averette, A.F., Kingsbury, J.M., Heitman, J., and Idnurm, A. (2016). Gene Function Analysis in the Ubiquitous Human Commensal and Pathogen Malassezia Genus. mBio *7*, e01853-16. https://doi.org/10.1128/mBio.01853-16.

31. Corzo-León, D.E., MacCallum, D.M., and Munro, C.A. (2020). Host Responses in an Ex Vivo Human Skin Model Challenged With Malassezia sympodialis. Front. Cell. Infect. Microbiol. *10*, 561382. https://doi.org/10.3389/fcimb.2020.561382.

32. Larson, P.J., Chong, D., Fleming, E., and Oh, J. (2021). Challenges in Developing a Human Model System for Skin Microbiome Research.

J. Invest. Dermatol. *141*, 228–231.e4. https://doi.org/10.1016/j.jid.2020.05.096.

33. Di Nardo, A., Chang, Y.-L., Alimohammadi, S., Masuda-Kuroki, K., Wang, Z., Sriram, K., and Insel, P.A. (2023). Mast cell tolerance in the skin microenvironment to commensal bacteria is controlled by fibroblasts. Cell Rep. *42*, 112453. https://doi.org/10.1016/j.celrep.2023.112453.

34. O'Sullivan, J.N., Rea, M.C., O'Connor, P.M., Hill, C., and Ross, R.P. (2019). Human skin microbiota is a rich source of bacteriocin-producing staphylococci that kill human pathogens. FEMS Microbiol. Ecol. *95*, fiy241. https://doi.org/10.1093/femsec/fiy241.

35. Joglekar, P., Conlan, S., Lee-Lin, S.-Q., Deming, C., Kashaf, S.S., Kong, H.H., Segre, J.A., Barnabas, B.B., Black, S., et al.; NISC Comparative Sequencing Program (2023). Integrated genomic and functional analyses of human skin-associated Staphylococcus reveal extensive inter- and intra-species diversity. Proc. Natl. Acad. Sci. USA *120*, e2310585120. https://doi.org/10.1073/pnas.2310585120.

36. Marrakchi, S., and Maibach, H.I. (2007). Biophysical parameters of skin: map of human face, regional, and age-related differences. Contact Dermatitis *57*, 28–34. https://doi.org/10.1111/j.1600-0536.2007.01138.x.

37. Lee, K., Zhang, I., Kyman, S., Kask, O., and Cope, E.K. (2020). Co-infection of Malassezia sympodialis With Bacterial Pathobionts Pseudomonas aeruginosa or Staphylococcus aureus Leads to Distinct Sinonasal Inflammatory Responses in a Murine Acute Sinusitis Model. Front. Cell. Infect. Microbiol. *10*, 472. https://doi.org/10.3389/fcimb.2020.00472.

38. Han, Y., Zhang, Y.J., Wang, H.X., Sun, Y.Z., Yang, Y., Li, Z.X., Qi, R.Q., and Gao, X.H. (2019). Malassezia furfur promoting growth of Staphylococcus epidermidis by increasing pH when cultured in a lipid-free environment. Chin. Med. J. (Engl) *132*, 873–876. https://doi.org/10.1097/CM9.0000000000000152.

39. Lyou, E.S., Kim, M.S., Kim, S.B., Park, M., Kim, K.D., Jung, W.H., and Lee, T.K. (2023). Single-cell phenotypes revealed as a key biomarker in bacterial–fungal interactions: a case study of Staphylococcus and Malassezia. Microbiol. Spectr. *11*, e0043723. https://doi.org/10.1128/spectrum.00437-23.

40. Applen Clancey, S., Ruchti, F., LeibundGut-Landmann, S., Heitman, J., and Ianiri, G. (2020). A Novel Mycovirus Evokes Transcriptional Rewiring in the Fungus Malassezia and Stimulates Beta Interferon Production in Macrophages. mBio *11*, e01534-20. https://doi.org/10.1128/mBio.01534-20.

41. Hurdle, J.G., O'Neill, A.J., Chopra, I., and Lee, R.E. (2011). Targeting bacterial membrane function: an underexploited mechanism for treating persistent infections. Nat. Rev. Microbiol. *9*, 62–75. https://doi.org/10.1038/nrmicro2474.

42. Angelova, M.I., Bitbol, A.-F., Seigneuret, M., Staneva, G., Kodama, A., Sakuma, Y., Kawakatsu, T., Imai, M., and Puff, N. (2018). pH sensing by lipids in membranes: The fundamentals of pH-driven migration, polarization and deformations of lipid bilayer assemblies. Biochim. Biophys. Acta Biomembr. *1860*, 2042–2063. https://doi.org/10.1016/j.bbamem.2018.02.026.

43. Parsons, J.B., Yao, J., Frank, M.W., Jackson, P., and Rock, C.O. (2012). Membrane Disruption by Antimicrobial Fatty Acids Releases Low-Molecular-Weight Proteins from Staphylococcus aureus. J. Bacteriol. *194*, 5294–5304. https://doi.org/10.1128/JB.00743-12.

44. Subramanian, C., Frank, M.W., Batte, J.L., Whaley, S.G., and Rock, C.O. (2019). Oleate hydratase from Staphylococcus aureus protects against palmitoleic acid, the major antimicrobial fatty acid produced by mammalian skin. J. Biol. Chem. *294*, 9285–9294. https://doi.org/10.1074/jbc.RA119.008439.

45. Gratani, F.L., Horvatek, P., Geiger, T., Borisova, M., Mayer, C., Grin, I., Wagner, S., Steinchen, W., Bange, G., Velic, A., et al. (2018). Regulation of the opposing (p)ppGpp synthetase and hydrolase activities in a bifunctional RelA/SpoT homologue from Staphylococcus aureus. PLoS Genet. *14*, e1007514. https://doi.org/10.1371/journal.pgen.1007514.

46. Horvatek, P., Salzer, A., Hanna, A.M.F., Gratani, F.L., Keinhörster, D., Korn, N., Borisova, M., Mayer, C., Rejman, D., Mäder, U., et al. (2020). Inducible expression of (pp)pGpp synthetases in Staphylococcus aureus is associated with activation of stress response genes. PLoS Genet. *16*, e1009282. https://doi.org/10.1371/journal.pgen.1009282.

47. Gentry, D., Li, T., Rosenberg, M., and McDevitt, D. (2000). The rel gene is essential for in vitro growth of Staphylococcus aureus. https://doi.org/10.1128/JB.182.17.4995-4997.2000.

48. Bryson, D., Hettle, A.G., Boraston, A.B., and Hobbs, J.K. (2020). Clinical Mutations That Partially Activate the Stringent Response Confer Multidrug Tolerance in Staphylococcus aureus. Antimicrob. Agents Chemother. *64*, e02103-19. https://doi.org/10.1128/AAC.02103-19.

49. Reiss, S., Pané-Farré, J., Fuchs, S., François, P., Liebeke, M., Schrenzel, J., Lindequist, U., Lalk, M., Wolz, C., Hecker, M., et al. (2012). Global analysis of the Staphylococcus aureus response to mupirocin. Antimicrob. Agents Chemother. *56*, 787–804. https://doi.org/10.1128/AAC.05363-11.

50. Hammer, B.K., and Swanson, M.S. (1999). Co-ordination of legionella pneumophila virulence with entry into stationary phase by ppGpp. Mol. Microbiol. *33*, 721–731. https://doi.org/10.1046/j.1365-2958.1999.01519.x.

51. Fritsch, V.N., Van Loi, V.V., Busche, T., Tung, Q.N., Lill, R., Horvatek, P., Wolz, C., Kalinowski, J., and Antelmann, H. (2020). The alarmone (p)ppGpp confers tolerance to oxidative stress during the stationary phase by maintenance of redox and iron homeostasis in Staphylococcus aureus. Free Radic. Biol. Med. *161*, 351–364. https://doi.org/10.1016/j.freeradbiomed.2020.10.322.

52. Aedo, S., and Tomasz, A. (2016). Role of the stringent stress response in the antibiotic resistance phenotype of methicillin-resistant staphylococcus aureus. Antimicrob. Agents Chemother. *60*, 2311–2317. https://doi.org/10.1128/AAC.02697-15.

53. Kim, C., Mwangi, M., Chung, M., Milheiriço, C., de Lencastre, H., and Tomasz, A. (2013). The Mechanism of Heterogeneous Beta-Lactam Resistance in MRSA: Key Role of the Stringent Stress Response. PLoS One *8*, e82814. https://doi.org/10.1371/journal.pone.0082814.

54. Gao, W., Chua, K., Davies, J.K., Newton, H.J., Seemann, T., Harrison, P.F., Holmes, N.E., Rhee, H.W., Hong, J.I., Hartland, E.L., et al. (2010). Two novel point mutations in clinical Staphylococcus aureus reduce linezolid susceptibility and switch on the stringent response to promote persistent infection. PLoS Pathog. *6*, e1000944. https://doi.org/10.1371/journal.ppat.1000944.

55. Chen, E., Shaffer, M.G., Bilodeau, R.E., West, R.E., Oberly, P.J., Nolin, T.D., and Culyba, M.J. (2023). Clinical rel mutations in Staphylococcus aureus prime pathogen expansion under nutrient stress. mSphere *8*, e0024923. https://doi.org/10.1128/msphere.00249-23.

56. Fang, M., and Bauer, C.E. (2018). Regulation of stringent factor by branched-chain amino acids. Proc. Natl. Acad. Sci. USA *115*, 6446–6451. https://doi.org/10.1073/pnas.1803220115.

57. Ronneau, S., Caballero-Montes, J., Coppine, J., Mayard, A., Garcia-Pino, A., and Hallez, R. (2019). Regulation of (p)ppGpp hydrolysis by a conserved archetypal regulatory domain. Nucleic Acids Res. *47*, 843–854. https://doi.org/10.1093/nar/gky1201.

58. Turnbull, K.J., Dzhygyr, I., Lindemose, S., Hauryliuk, V., and Roghanian, M. (2019). Intramolecular Interactions Dominate the Autoregulation of Escherichia coli Stringent Factor RelA. Front. Microbiol. *10*, 1966. https://doi.org/10.3389/fmicb.2019.01966.

59. Patra, M., Salonen, E., Terama, E., Vattulainen, I., Faller, R., Lee, B.W., Holopainen, J., and Karttunen, M. (2006). Under the Influence of Alcohol: The Effect of Ethanol and Methanol on Lipid Bilayers. Biophys. J. *90*, 1121–1135. https://doi.org/10.1529/biophysj.105.062364.

60. Brauner, A., Fridman, O., Gefen, O., and Balaban, N.Q. (2016). Distinguishing between resistance, tolerance and persistence to antibiotic treatment. Nat. Rev. Microbiol. *14*, 320–330. https://doi.org/10.1038/nrmicro.2016.34.

61. Brauner, A., Shoresh, N., Fridman, O., and Balaban, N.Q. (2017). An Experimental Framework for Quantifying Bacterial Tolerance. Biophys. J. *112*, 2664–2671. https://doi.org/10.1016/j.bpj.2017.05.014.

62. Pohl, K., Francois, P., Stenz, L., Schlink, F., Geiger, T., Herbert, S., Goerke, C., Schrenzel, J., and Wolz, C. (2009). CodY in Staphylococcus aureus: a Regulatory Link between Metabolism and Virulence Gene Expression. J. Bacteriol. *191*, 2953–2963. https://doi.org/10.1128/JB.01492-08.

63. Giachino, P., Engelmann, S., and Bischoff, M. (2001). ς B Activity Depends on RsbU in Staphylococcus aureus. J. Bacteriol. *183*, 1843–1852. https://doi.org/10.1128/JB.183.6.1843-1852.2001.

64. Ranganathan, N., Johnson, R., and Edwards, A.M. (2020). The general stress response of Staphylococcus aureus promotes tolerance of antibiotics and survival in whole human blood. Microbiology (NY) *166*, 1088–1094. https://doi.org/10.1099/mic.0.000983.

65. Underhill, D.M., and Iliev, I.D. (2014). The mycobiota: interactions between commensal fungi and the host immune system. Nat. Rev. Immunol. *14*, 405–416. https://doi.org/10.1038/nri3684.

66. Erb Downward, J.R., Falkowski, N.R., Mason, K.L., Muraglia, R., and Huffnagle, G.B. (2013). Modulation of Post-Antibiotic Bacterial Community Reassembly and Host Response by Candida albicans. Sci. Rep. *3*, 2191. https://doi.org/10.1038/srep02191.

67. Ott, S.J., Kühbacher, T., Musfeldt, M., Rosenstiel, P., Hellmig, S., Rehman, A., Drews, O., Weichert, W., Timmis, K.N., and Schreiber, S. (2008). Fungi and inflammatory bowel diseases: Alterations of composition and diversity. Scand. J. Gastroenterol. *43*, 831–841. https://doi.org/10.1080/00365520801935434.

68. Markey, L., Shaban, L., Green, E.R., Lemon, K.P., Mecsas, J., and Kumamoto, C.A. (2018). Pre-colonization with the commensal fungus Candida albicans reduces murine susceptibility to Clostridium difficile infection. Gut Microbes *9*, 497–509. https://doi.org/10.1080/19490976.2018.1465158.

69. Pierce, E.C., Morin, M., Little, J.C., Liu, R.B., Tannous, J., Keller, N.P., Pogliano, K., Wolfe, B.E., Sanchez, L.M., and Dutton, R.J. (2021). Bacterial–fungal interactions revealed by genome-wide analysis of bacterial mutant fitness. Nat. Microbiol. *6*, 87–102. https://doi.org/10.1038/s41564-020-00800-z.

70. Kastman, E.K., Kamelamela, N., Norville, J.W., Cosetta, C.M., Dutton, R.J., and Wolfe, B.E. (2016). Biotic Interactions Shape the Ecological Distributions of Staphylococcus Species. mBio *7*, e01157-16. https://doi.org/10.1128/mBio.01157-16.

71. Ianiri, G., LeibundGut-Landmann, S., and Dawson, T.L. (2022). Malassezia: A Commensal, Pathogen, and Mutualist of Human and Animal Skin. Annu. Rev. Microbiol. *76*, 757–782. https://doi.org/10.1146/annurev-micro-040820-010114.

72. Donnarumma, G., Perfetto, B., Paoletti, I., Oliviero, G., Clavaud, C., Del Bufalo, A., Guéniche, A., Jourdain, R., Tufano, M.A., and Breton, L. (2014). Analysis of the response of human keratinocytes to Malassezia globosa and restricta strains. Arch. Dermatol. Res. *306*, 763–768. https://doi.org/10.1007/s00403-014-1479-1.

73. Baroni, A., Orlando, M., Donnarumma, G., Farro, P., Iovene, M.R., Tufano, M.A., and Buommino, E. (2006). Toll-like receptor 2 (TLR2) mediates intracellular signalling in human keratinocytes in response to Malassezia furfur. Arch. Dermatol. Res. *297*, 280–288. https://doi.org/10.1007/s00403-005-0594-4.

74. Zhang, E., Tanaka, T., Tajima, M., Tsuboi, R., Nishikawa, A., and Sugita, T. (2011). Characterization of the skin fungal microbiota in patients with atopic dermatitis and in healthy subjects. Microbiol. Immunol. *55*, 625–632. https://doi.org/10.1111/j.1348-0421.2011.00364.x.

75. Wilde, P.F., and Stewart, P.S. (1968). A study of the fatty acid metabolism of the yeast Pityrosporum ovale. Biochem. J. *108*, 225–231. https://doi.org/10.1042/bj1080225.

76. Caballero-Flores, G., Pickard, J.M., and Núñez, G. (2023). Microbiota-mediated colonization resistance: mechanisms and regulation. Nat. Rev. Microbiol. *21*, 347–360. https://doi.org/10.1038/s41579-022-00833-7.

77. Kengmo Tchoupa, A., Kretschmer, D., Schittek, B., and Peschel, A. (2023). The epidermal lipid barrier in microbiome-skin interaction. Trends Microbiol. *31*, 723–734. https://doi.org/10.1016/j.tim.2023.01.009.

78. Guzior, D.V., and Quinn, R.A. (2021). Review: microbial transformations of human bile acids. Microbiome *9*, 140. https://doi.org/10.1186/s40168-021-01101-1.

79. Eberlein-König, B., Schäfer, T., Huss-Marp, J., Darsow, U., Möhrenschlager, M., Herbert, O., Abeck, D., Krämer, U., Behrendt, H., and Ring, J. (2000). Skin surface pH, stratum corneum hydration, trans-epidermal water loss and skin roughness related to atopic eczema and skin dryness in a population of primary school children. Acta Derm. Venereol. *80*, 188–191. https://doi.org/10.1080/000155500750042943.

80. Kobayashi, T., Glatz, M., Horiuchi, K., Kawasaki, H., Akiyama, H., Kaplan, D.H., Kong, H.H., Amagai, M., and Nagao, K. (2015). Dysbiosis and Staphylococcus aureus Colonization Drives Inflammation in Atopic Dermatitis. Immunity *42*, 756–766. https://doi.org/10.1016/j.immuni.2015.03.014.

81. Kuiack, R.C., Veldhuizen, R.A.W., and McGavin, M.J. (2020). Novel Functions and Signaling Specificity for the GraS Sensor Kinase of Staphylococcus aureus in Response to Acidic pH. J. Bacteriol. *202*, e00219-20. https://doi.org/10.1128/JB.00219-20.

82. Marsman, G., Zheng, X., Čerina, D., Lacey, K.A., Liu, M., Humme, D., Goosmann, C., Brinkmann, V., Harbort, C.J., Torres, V.J., et al. (2024). Histone H1 kills MRSA. Cell Rep. *43*, 114969. https://doi.org/10.1016/j.celrep.2024.114969.

83. Nakatsuji, T., Chen, T.H., Narala, S., Chun, K.A., Two, A.M., Yun, T., Shafiq, F., Kotol, P.F., Bouslimani, A., Melnik, A.V., et al. (2017). Antimicrobials from human skin commensal bacteria protect against Staphylococcus aureus and are deficient in atopic dermatitis. Sci. Transl. Med. *9*, eaah4680. https://doi.org/10.1126/scitranslmed.aah4680.

84. Hackel, M.A., Tsuji, M., Yamano, Y., Echols, R., Karlowsky, J.A., and Sahm, D.F. (2019). Reproducibility of broth microdilution MICs for the novel siderophore cephalosporin, cefiderocol, determined using iron-depleted cation-adjusted Mueller-Hinton broth. Diagn. Microbiol. Infect. Dis. *94*, 321–325. https://doi.org/10.1016/j.diagmicrobio.2019.03.003.

85. Kuiack, R.C., Tuffs, S.W., Dufresne, K., Flick, R., McCormick, J.K., and McGavin, M.J. (2023). The fadXDEBA locus of Staphylococcus aureus is required for metabolism of exogenous palmitic acid and in vivo growth. Mol. Microbiol. *120*, 425–438. https://doi.org/10.1111/mmi.15131.

86. Parsons, J.B., Broussard, T.C., Bose, J.L., Rosch, J.W., Jackson, P., Subramanian, C., and Rock, C.O. (2014). Identification of a two-component fatty acid kinase responsible for host fatty acid incorporation by Staphylococcus aureus. Proc. Natl. Acad. Sci. USA *111*, 10532–10537. https://doi.org/10.1073/pnas.1408797111.

87. Ledger, E.V.K., Mesnage, S., and Edwards, A.M. (2022). Human serum triggers antibiotic tolerance in Staphylococcus aureus. Nat. Commun. *13*, 2041. https://doi.org/10.1038/s41467-022-29717-3.

88. Rowe, S.E., Wagner, N.J., Li, L., Beam, J.E., Wilkinson, A.D., Radlinski, L.C., Zhang, Q., Miao, E.A., and Conlon, B.P. (2020). Reactive oxygen species induce antibiotic tolerance during systemic Staphylococcus aureus infection. Nat. Microbiol. *5*, 282–290. https://doi.org/10.1038/s41564-019-0627-y.

89. Stewart, P.S. (2015). Antimicrobial Tolerance in Biofilms. Microbiol. Spectr. *3*. https://doi.org/10.1128/microbiolspec.MB-0010-2014.

90. Harriott, M.M., and Noverr, M.C. (2009). Candida albicans and Staphylococcus aureus Form Polymicrobial Biofilms: Effects on Antimicrobial Resistance. Antimicrob. Agents Chemother. *53*, 3914–3922. https://doi.org/10.1128/AAC.00657-09.

91. Nabb, D.L., Song, S., Kluthe, K.E., Daubert, T.A., Luedtke, B.E., and Nuxoll, A.S. (2019). Polymicrobial Interactions Induce Multidrug Tolerance in Staphylococcus aureus Through Energy Depletion. Front. Microbiol. *10*, 2803. https://doi.org/10.3389/fmicb.2019.02803.

92. Koch, G., Yepes, A., Förstner, K.U., Wermser, C., Stengel, S.T., Modamio, J., Ohlsen, K., Foster, K.R., and Lopez, D. (2014). Evolution of Resistance to a Last-Resort Antibiotic in Staphylococcus aureus via Bacterial Competition. Cell *158*, 1060–1071. https://doi.org/10.1016/j.cell.2014.06.046.

93. Gioti, A., Nystedt, B., Li, W., Xu, J., Andersson, A., Averette, A.F., Münch, K., Wang, X., Kappauf, C., Kingsbury, J.M., et al. (2013). Genomic insights into the atopic eczema-associated skin commensal yeast Malassezia sympodialis. mBio *4*, e00572–e00512. https://doi.org/10.1128/mBio.00572-12.

94. Monk, I.R., Shah, I.M., Xu, M., Tan, M.-W., and Foster, T.J. (2012). Transforming the untransformable: application of direct transformation to manipulate genetically Staphylococcus aureus and Staphylococcus epidermidis. mBio *3*, e00277-11. https://doi.org/10.1128/mBio.00277-11.

95. de Jong, N.W.M., van der Horst, T., van Strijp, J.A.G., and Nijland, R. (2017). Fluorescent reporters for markerless genomic integration in Staphylococcus aureus. Sci. Rep. *7*, 43889. https://doi.org/10.1038/srep43889.

96. Deatherage, D.E., and Barrick, J.E. (2014). Identification of Mutations in Laboratory-Evolved Microbes from Next-Generation Sequencing Data Using breseq. In Engineering and Analyzing Multicellular Systems. Methods and Protocols, L. Sun, and W. Shou, eds. (Springer), pp. 165–188. https://doi.org/10.1007/978-1-4939-0554-6_12.

97. Dührkop, K., Fleischauer, M., Ludwig, M., Aksenov, A.A., Melnik, A.V., Meusel, M., Dorrestein, P.C., Rousu, J., and Böcker, S. (2019). SIRIUS 4: a rapid tool for turning tandem mass spectra into metabolite structure information. Nat. Methods *16*, 299–302. https://doi.org/10.1038/s41592-019-0344-8.

98. Chambers, M.C., Maclean, B., Burke, R., Amodei, D., Ruderman, D.L., Neumann, S., Gatto, L., Fischer, B., Pratt, B., Egertson, J., et al. (2012). A cross-platform toolkit for mass spectrometry and proteomics. Nat. Biotechnol. *30*, 918–920. https://doi.org/10.1038/nbt.2377.

99. Schmid, R., Heuckeroth, S., Korf, A., Smirnov, A., Myers, O., Dyrlund, T.S., Bushuiev, R., Murray, K.J., Hoffmann, N., Lu, M., et al. (2023). Integrative analysis of multimodal mass spectrometry data in MZmine 3. Nat. Biotechnol. *41*, 447–449. https://doi.org/10.1038/s41587-023-01690-2.

100. Reed, P., Atilano, M.L., Alves, R., Hoiczyk, E., Sher, X., Reichmann, N.T., Pereira, P.M., Roemer, T., Filipe, S.R., Pereira-Leal, J.B., et al. (2015). Staphylococcus aureus Survives with a Minimal Peptidoglycan Synthesis Machine but Sacrifices Virulence and Antibiotic Resistance. PLoS Pathog. *11*, e1004891. https://doi.org/10.1371/journal.ppat.1004891.

101. Löfblom, J., Kronqvist, N., Uhlén, M., Ståhl, S., and Wernérus, H. (2007). Optimization of electroporation-mediated transformation: Staphylococcus carnosus as model organism. J. Appl. Microbiol. *102*, 736–747. https://doi.org/10.1111/j.1365-2672.2006.03127.x.

102. Corrigan, R.M., Bowman, L., Willis, A.R., Kaever, V., and Gründling, A. (2015). Cross-talk between Two Nucleotide-signaling Pathways in Staphylococcus aureus. J. Biol. Chem. *290*, 5826–5839. https://doi.org/10.1074/jbc.M114.598300.

Please cite this article in press as: Kowalski et al., Skin mycobiota-mediated antagonism against *Staphylococcus aureus* through a modified fatty acid, Current Biology (2025), https://doi.org/10.1016/j.cub.2025.03.055

STAR★METHODS

KEY RESOURCES TABLE

REAGENT or RESOURCE	SOURCE	IDENTIFIER
Bacterial and virus strains		
Staphylococcus aureus NRS193, MRSA 2	BEI Resources	NR-45992
Staphylococcus aureus Je2, MRSA 1	BEI Resources	NR-46543
Staphylococcus aureus HFH-29568, MRSA 3	BEI Resources	NR-10186
Staphylococcus aureus HFH-30364, MRSA 4	BEI Resources	NR-10189
Staphylococcus aureus SR2609, MRSA 5	BEI Resources	NR-50507
Staphylococcus aureus RN4850, MSSA 1	BEI Resources	NR-45955
Staphylococcus aureus WKZ-1, MSSA 2	BEI Resources	NR-28984
Staphylococcus aureus MN8, MSSA 3	BEI Resources	NR-45918
Staphylococcus aureus 880 BR-VRSA, VRSA	BEI Resources	NR-49120
Staphylococcus aureus IL (Isolate F), VISA 1	BEI Resources	NR-45905
Staphylococcus aureus LIM2, VISA 2	BEI Resources	NR-45881
Escherichia coli Nissle	Gifted by K. Guillemin	N/A
Staphylococcus hominis SK119, Sho 1	BEI Resources	HM-119
Staphylococcus hominis VCU122, Sho 2	BEI Resources	NR-46399
Staphylococcus capitis SK14, Scap 1	BEI Resources	HM-117
Staphylococcus capitis VCU116, Scap 2	BEI Resources	NR-46394
Staphylococcus epidermidis NIHLM001, Sepi 1	BEI Resources	HM-896
Staphylococcus epidermidis NIHLM040, Sepi 4	BEI Resources	HM-912
Staphylococcus epidermidis NIHLM015, Sepi 2	BEI Resources	HM-901
Staphylococcus epidermidis NIHLM020, Sepi 3	BEI Resources	HM-904
Staphylococcus epidermidis SK135, Sepi 5	BEI Resources	HM-118
Staphylococcus epidermidis W23144, Sepi 6	BEI Resources	HM-142
Escherichia coli K-12 DC10B	BEI Resources	NR-49804
Staphylococcus aureus Fluorescent Reporter Plasmid pSRFPS1	BEI Resources	NR-51164
Je2, transposon mutant NE1555 (codY::Tn)	BEI Resources	NR-48097
Malassezia sympodialis Simmons et Guého	ATCC	ATCC42132
Malassezia furfur (Robin) Baillon	ATCC	ATCC44344
Malassezia globosa Midgley, E. Guého et J. Guilot	ATCC	MYA-4612
Malassezia restricta E. Guého, J. Guillot et Midgley	ATCC	MYA-4611
Malassezia sympodialis KS013	Gioti et al.[93]	N/A
Malassezia sympodialis KS014	Gioti et al.[93]	N/A
Malassezia sympodialis KS269	Gioti et al.[93]	N/A
Malassezia sympodialis KS270	Gioti et al.[93]	N/A
Malassezia pachydermatis	Gifted by J. Heitman	N/A
Malassezia furfur 10086	Gifted by J. Heitman	N/A
Staphylococcus aureus NRS193, EVOL-A	This paper	N/A
Staphylococcus aureus NRS193, EVOL-B	This paper	N/A
Staphylococcus aureus NRS193, EVOL-C	This paper	N/A
Staphylococcus aureus NRS193, EVOL-D	This paper	N/A
Staphylococcus aureus NRS193, EVOL-A ΔmecA	This paper	N/A
Staphylococcus aureus NRS193, $WT^{Rel\text{-}A}$	This paper	N/A
Staphylococcus aureus NRS193, $WT^{Rel\text{-}D}$	This paper	N/A
Staphylococcus aureus NRS193, EVOL-$A^{Rel\text{-}WT}$	This paper	N/A
Staphylococcus aureus NRS193, EVOL-$D^{Rel\text{-}WT}$	This paper	N/A

(*Continued on next page*)

Please cite this article in press as: Kowalski et al., Skin mycobiota-mediated antagonism against *Staphylococcus aureus* through a modified fatty acid, Current Biology (2025), https://doi.org/10.1016/j.cub.2025.03.055

Continued

REAGENT or RESOURCE	SOURCE	IDENTIFIER
Staphylococcus aureus NRS193, WT^{F128Y}	This paper	N/A
Staphylococcus aureus NRS193, WT^{A567*}	This paper	N/A
Staphylococcus aureus NRS193, WT^{E657*}	This paper	N/A
Staphylococcus aureus NRS193, $WT^{\Delta 11bp,\ 658*}$	This paper	N/A
Staphylococcus aurues NRS193, *S. aureus*^{GFP}	This paper	N/A
Staphylococcus aureus HFH-29568, USA300 CFS^{R}	This paper	N/A
Staphylococcus aureus NRS193, ΔcodY	This paper	N/A
Staphylococcus aureus NRS193, EVOL-A ΔcrtM	This paper	N/A
Staphylococcus aureus NRS193, WT Pasp23-YFP	This paper	N/A
Staphylococcus aureus NRS193, EVOL-A Pasp23-YFP	This paper	N/A
Staphylococcus aureus NRS193, EVOL-A ΔsigB Pasp23-YFP	This paper	N/A
Staphylococcus aureus NRS193, EVOL-A ΔsigB	This paper	N/A
Staphylococcus aureus NRS193, WT^{F128Y} Pasp23-YFP	This paper	N/A
Staphylococcus aureus NRS193, WT^{E657*} Pasp23-YFP	This paper	N/A
Staphylococcus aureus NRS193, WT^{F128Y} ΔsigB	This paper	N/A
Staphylococcus aureus NRS193, WT^{E657*} ΔsigB	This paper	N/A
Staphylococcus aureus NRS193, ΔsigB	This paper	N/A
Biological samples		
Human skin biopsies: NativeSkin access 11 mm – Custom (no antifungals or antibiotics)	Genoskin	N/A
Chemicals, peptides, and recombinant proteins		
Tryptic Soy Agar (TSA)	BD Difco	Cat# 236950
Tryptic Soy Broth (TSB)	BD Difco	Cat# 211822
Potato Dextrose Broth (PDB)	Sigma-Aldrich	Cat# P6685
Potato Dextrose Agar (PDA)	Sigma-Aldrich	Cat# 70139
Lysogeny Broth (LB)	Fisher Scientific	Cat# 611895000
Ampicillin	Sigma-Aldrich	Cat# A9518
Chloramphenicol	Sigma-Aldrich	Cat# C0857
Anhydrotetracycline hydrochloride	Sigma-Aldrich	Cat# 37919
Synthetic sebum	Fisher Scientific	Cat# NC1769280
Malt Extract		N/A
Ox-Bile, dehydrated	Sigma-Aldrich; HiMedia Laboratories	Cat# 70168; Cat# CR010
Tween40, viscous liquid	Sigma-Aldrich	Cat# P1504
Tween20	Fisher Scientific	Cat# BP337
Peptone	Sigma-Aldrich	Cat# 70173
Glycerol	Sigma-Aldrich	Cat# G7757
Oleic Acid	Millipore Sigma	Cat# 364525
Agar	BD Difco	Cat# DF0882
Tween60, nonionic	Sigma-Aldrich	Cat# P1629
Glycerol monostearate	Spectrum Chemical	Cat# GL149
M9 Minimal Salts	Sigma-Aldrich	Cat# M6030
Dextrose	Fisher Scientific	Cat# D16500
Casamino acids	Research Products International	Cat# C45000
$MgSO_4$	Sigma-Aldrich	Cat# 208094
$CaCl_2$	Sigma-Aldrich	Cat# C4901
Calcium pentothenate	Acros Organics	Cat# 2433000
Thiamine-HCl	Cayman Chemical	Cat# 25656

(*Continued on next page*)

Please cite this article in press as: Kowalski et al., Skin mycobiota-mediated antagonism against *Staphylococcus aureus* through a modified fatty acid, Current Biology (2025), https://doi.org/10.1016/j.cub.2025.03.055

Continued

REAGENT or RESOURCE	SOURCE	IDENTIFIER
Nicotinamide	Thermo Fisher	Cat# J60387
Tween80, viscous liquid	Sigma-Aldrich	Cat# P1754
PBS	Sigma-Aldrich	Cat# 11666789
Calcofluor white (Fluorescent Brightener 28)	MP Biomedicals	Cat# 0215806701
Dithiothreitol	Thermo Fisher	Cat# R0861
Proteinase K	Thermo Fisher	Cat# EO0491
Propodium iodine	Sigma-Aldrich	Cat# P4170
DMSO	EMD Millipore	Cat# 317275
Lysostaphin	Sigma-Aldrich	Cat# L9043; SAE0091
Mupirocin	Selleck Chemicals	Cat# S4297
Oxacillin	Sigma-Aldrich	Cat# O1002
Phusion polymerase	NEB	Cat# M0530S
T4 Polynucleotide Kinase	NEB	Cat# M0201S
SmaI	NEB	Cat# R0141S
EcoRV	NEB	Cat# R0195L
XbaI	NEB	Cat# R0145S
Novagen Pellet Paint Co-precipitant	EMB Millipore	Cat# 69049-3
Quick Ligation Kit	NEB	Cat# M2200L
Shrimp Alkaline Phosphatase	NEB	Cat# M0371L
Mueller-Hinton Broth	Sigma-Aldrich	Cat# 70192
Vancomycin	Cayman Chemical	Cat# 15327
Daptomycin	Selleck Chemicals	Cat# S1373
Ciprofloxacin	Sigma-Aldrich	Cat# 17850
2-hydroxy hexadecanoic acid	Ambeed Inc.	Cat# A621632
3-hydroxy hexadecanoic acid	Cayman Chemicals	Cat# 19934
4-hydroxy hexadecanoic acid	Ambeed Inc.	Cat# A1505121
7-hydroxy hexadecanoic acid	Ambeed Inc.	Cat# A150507
9-hydroxy hexadecanoic acid	Ambeed Inc.	Cat# A150507
10-hydroxy hexadecanoic acid	Ambeed Inc.	Cat# A1165700
11-hydroxy hexadecanoic acid	TargetMol	Cat# T32253
16-hydroxy hexadecanoic acid	Sigma-Aldrich	Cat# 177490
Critical commercial assays		
BacTiter Glo™ Microbial Cell Viability Assay	Promega	Cat# G8230
Qiagen DNeasy Blood and Tissue kit	Qiagen	Cat# 69504
Zymo DNA Clean Concentrator kit	Zymo Research	Cat# D4004
Zymopure II Plasmid Midiprep kit	Zymo Research	Cat# D4201
Q5 Site-Directed-Mutagenesis kit	NEB	Cat# E0552S
Deposited data		
S. aureus NRS193 genome sequence	NCBI	GenBank: GCA_045348275.1
DNA sequence reads from evolved *S. aureus*	NCBI	BioProject: PRJNA1107622
Oligonucleotides		
See Table S3 for primers	IDT	N/A
Recombinant DNA		
pIMAY	Monk et al.[94]	Addgene plasmid #68939
pTH3	de Jong et al.[95]	Addgene plasmid #84453
pGFP-pH	This paper	N/A
pRel-swap	This paper	N/A

(*Continued on next page*)

Please cite this article in press as: Kowalski et al., Skin mycobiota-mediated antagonism against *Staphylococcus aureus* through a modified fatty acid, Current Biology (2025), https://doi.org/10.1016/j.cub.2025.03.055

Continued

REAGENT or RESOURCE	SOURCE	IDENTIFIER
Software and algorithms		
breseq	Deatherage and Barrick[96]	RRID: SCR_01081
GraphPad Prism 10	GraphPad	RRID: SCR_002798
SnapGene	SnapGene	RRID: SCR_015052
NIS-Elements	Nikon	RRID: SCR_014329
Gen5	Agilent	RRID: SCR_017317
SIRIUS 5	Dührkop et al.[97]	https://bio.informatik.uni-jena.de/software/sirius/
MSconvert	Chambers et al.[98]	https://bio.tools/msconvert
MZmine3	Schmid et al.[99]	https://github.com/mzmine/
ImageQuant TL	Cytiva	RRID: SCR_018374
Microsoft Excel	Microsoft	RRID: SCR_016137
Other		
Mattek 35 mm Dish, No. 1.5 coverslip, uncoated	MatTek Cooperation	Cat# P35G-1.5-10-C
Black-walled 96 well paltes	Corning	Cat# 3601
PEI-cellulose F thin-layer chromatography (TLC) plates	Merck Millipore	Cat# 105579
Syringe filter: MCE membrane (0.22 μm)	Fisher Scientific	Cat# SLGL0250S
10 kDa MWCO spin column	Thermo Fisher	Cat# 88517

EXPERIMENTAL MODEL AND STUDY PARTICIPANT DETAILS

Healthy human skin biopsies were sourced as NativeSkin Access 11mm biopsies from Genoskin (Salem, MA, USA). Genoskin represents the widest network of IRB-approved skin sourcing across Europe and the United States. The biopsies are prepared from discarded tissue following surgery and collected with patient informed consent in respect of the Declaration of Helsinki and approval of the French Ministry of Research and Higher Education and French Ethics Committee. The use of NativeSkin human skin biopsies falls within the category of 'unidentifiable biospecimens obtained from a provider' and are not considered human subject research. All biopsies obtained for this study were from abdominal skin of female donors. Skin from males was not included because most available tissue is from female patients, and this is a limitation of this study. Biopsies are embedded in a matrix and maintained with culture media that is free of antibiotics and antifungals. Biopsies remain viable at 37°C with 5% CO2 for up to 10 days according to the provided protocols.

METHOD DETAILS

Bacterial and yeast culture conditions

S. aureus and other staphylococci were maintained on tryptic soy agar (TSA) or broth (TSB) at 37°C. Unless otherwise noted, staphylococci were cultured overnight to stationary phase (~16-h) and sub-cultured 1:10 in TSB for 1-h corresponding to early exponential phase. The wild type (WT) *S. aureus* strain used in this study is the ST1, USA400 isolate NRS193. This isolate was selected because it did not originate from a skin infection, is available through BEI Resources, and is closely related to the USA400 reference strain MW2. The sequenced and annotated genome for NRS193 has been deposited in NCBI as part of this study (GenBank: GCA_045348275.1). *E. coli* strains were maintained in LB with antibiotic as needed: 100 μg/mL ampicillin or 25 μg/mL chloramphenicol. *S. aureus* was cultured with 10 μg/mL chloramphenicol when necessary.

Malassezia species were maintained on mDixon media (36 g/L Malt Extract, 20 g/L Ox-bile, 10 mL/L Tween40, 6g/L peptone (from casein and other animal proteins), 2 mL/L glycerol, 2 mL/L oleic acid, 15 g/L agar, adjusted to pH 6 with HCl). Some experiments were performed with Ox-Bile sourced from Hi-Media, and this was used at 10 g/L. For *M. globosa* and *M. restricta*, Tween60 replaced Tween40 and 0.5 g/L glycerol monostearate was added. All *Malassezia* were grown at 30°C. Unless otherwise noted the strain of *M. sympodialis* used is KS269.[93] When noted mPDA (modified potato dextrose agar) was utilized and contains PDA with 4g/L Ox-bile (2 g/L Hi-Media), 4 mL/L Tween60, and 1 mL/L Tween20 as previously described.[30] For modified potato dextrose broth (mPDB), the recipe was the same as mPDA except mPDB base was used. Synthetic sebum media is based on SSM9PR media described previously with 0.1% synthetic sebum.[100] It was prepared as follows: 11.28g/L M9 Salts, 10 g/L dextrose, 10 g/L casamino acids, 2 mM $MgSO_4$, 0.1 mM $CaCl_2$, 1 mg/L calcium pantothenate, 1 mg/L thiamine-HCl, 1 mg/mL nicotinamide, 1 mL/L synthetic sebum, 3 mL/L Tween80. Tween80 and synthetic sebum were first mixed 3:1 and autoclaved separately. Ms-CFS collected from the synthetic sebum was after 120-h of *M. sympodialis* KS269 growth.

Please cite this article in press as: Kowalski et al., Skin mycobiota-mediated antagonism against *Staphylococcus aureus* through a modified fatty acid, Current Biology (2025), https://doi.org/10.1016/j.cub.2025.03.055

Adjacent colony assay and mixed biofilms

For adjacent colony assays, *Malassezia* species were collected from a 96-h culture from 30°C and washed in fresh mDixon media. The OD_{600} was adjusted to 1 and 10 μL was spotted in triplicate on mDixon agar and incubated at 30°C for 72-h. *S. aureus* NRS193 or *S. hominis* SK119 were cultured overnight in TSB and subcultured as described above before cells were pelleted and resuspended in mDixon. The OD_{600} was adjusted to 0.1 in mDixon, and 10 μL was spotted adjacent to the 72-h *Malassezia* colonies. Plates were returned to 30°C for 24-h and then photographed. The protocol was similar for *E. coli*, except it was grown in LB. Representative images shown from a minimum of three independent experiments.

For mixed biofilm assays *S. aureus* and *Malassezia* were prepared similarly as above but were adjusted to OD_{600} of 0.2 and 2 in mDixon respectively. For the co-culture condition, *S. aureus* and *M. sympodialis* were mixed 1:1 and 15 μL was spotted on mDixon agar. For monoculture conditions, *S. aureus* was mixed 1:1 with mDixon (final OD_{600}=0.1) and 15 μL was spotted on mDixon agar. Plates were incubated for 6 days at 30°C, after which entire colony biofilms were scraped up and resuspended in 500 μL of mDixon. After vigorous vortexing (maximum power, 1 min.) to disrupt aggregates, the suspension was serially diluted to plate for *S. aureus* viable counts on TSA at 37°C. When performed with mPDA, the protocol was the same except mDixon broth and agar were replaced by mPDB and mPDA respectively. Data points indicate individual biofilms from three independent experiments.

Co-colonization of human skin biopsies

M. sympodialis KS269 cells were grown at 30°C for 72-h in mDixon, washed twice with sterile PBS and resuspended in PBS with 10 μg/mL calcofluor white (CFW) for 30 min. at room temperature with agitation. We confirmed this concentration of CFW was nontoxic as yeast viable counts do not decrease after labeling (Figure S1B). Yeast were pelleted, resuspended in PBS, and enumerated with a hemocytometer. $5x10^5$ yeast were inoculated per biopsy in 10 μL of PBS. Control biopsies received 10 μL of PBS. After 6-days of incubation at 37°C, 5% CO_2, *S. aureus* expressing GFP was inoculated as follows. *S. aureus* constitutively expressing GFP on a plasmid was cultured in TSB with 10 μg/mL chloramphenicol to stationary phase and then subcultured 1:10 for 1-h in the same conditions. Cells were washed twice in PBS and resuspended in PBS with 10 μg/mL chloramphenicol at an OD_{600}=0.5 that corresponds to ~$5x10^6$ CFUs/10 μL inoculum. Each biopsy was inoculated with 10 μL *S. aureus* suspension. After 24-h at 37°C, 5% CO_2, one biopsy from each group was removed from the transwell and O-ring with sterile tweezers and inverted into a MatTek glass bottom imaging dish with 200 μL of PBS. Biopsies could then be imaged on an inverted Nikon CSU-W1 SoRa spinning disk microscope using NIS-Elements software. The skin surface is auto- fluorescent with 561 nm excitation which was used to locate the skin surface. The CFW-labeled yeast were visible with excitation at 405 nm and *S. aureus*^{GFP} was visible with excitation at 488nm. Imaging was performed with a 40X water immersion objective. Max projection images were generated in NIS-Elements.

To collect CFUs from the skin biopsies, skin was removed from the transwell and O-ring with sterile tweezers. Sterile scissors were used to cut the skin into four pieces. Skin pieces were placed in 1 mL sterile PBS and vortexed at maximum speed for 3 min. to disrupt the attached microorganisms. Biopsies were then shaken at 250 rpm for 2-h after which they were again vortexed at maximum speed for 2 min. The disrupted skin is allowed to settle briefly, and the PBS is removed, diluted, and plated on TSA for *S. aureus* CFUs. Percent colonization is calculated based on recovered *S. aureus* CFUs relative to the calculated inoculum. The experiment was repeated with biopsies from 4 separate donors. All skin biopsies were from female abdominal tissue.

S. aureus competition on human skin biopsies

For competition experiments, skin biopsies were colonized with unlabeled *M. sympodialis* KS269 or PBS as the vehicle control for 6 days as described above before inoculation with *S. aureus*. *S. aureus* was inoculated as a 1:1 mixture of WT (NRS193) to EVOL-D cells prepared as described above for the co-culturing experiments on skin biopsies. After 24-h, biopsies were disrupted and recovered *S. aureus* CFUs were serially diluted and plated on TSA. Plates were incubated at 37°C for 24-h and then room temperature for 24-h to allow the colony pigmentation to develop. Smaller bright yellow colonies corresponded to EVOL-D, where larger white colonies corresponded to WT. The same 1:1 strain mixtures were also treated *in vitro* with 30% Ms-CFS for 2-h and plated in the same manner to differentiate colony morphotypes.

CFS preparation and treatment

Five to 10 large *M. sympodialis* colonies from a 72-h mDixon agar plate were used to inoculate mDixon broth. Cultures were incubated at 30°C with shaking at 200 rpm for 96-h. Yeast were pelleted for 2 min. at 5000 rcf and the supernatant decanted. The pH where noted was adjusted to the desired pH with HCl or NaOH. A pH matched media control was also generated. Both media control and supernatant were filter-sterilized with a syringe tip filter through a 0.22 μm MCE filter. This sterilized cell-free supernatant (CFS) and control media were stored at 4°C and before use in experiments were warmed in a 37°C water bath for 10 min.

Unless otherwise noted, all experiments were performed with 50% CFS that was generated by mixing the CFS 1:1 with the pH matched media control. *S. aureus* and other staphylococci were cultured as described above in TSB before cells were pelleted and resuspended in mDixon (pH 6). *S. aureus* and other staphylococci were inoculated into the 50% CFS or pH-matched controls at a final OD_{600}=0.02. After treatment, cells were serially diluted and plated on TSA to calculate viability.

Treatment of human skin biopsies

S. aureus expressing red fluorescent protein (RFP) on a plasmid (*S. aureus*^{RFP}) and shown to be sensitive to *M. sympodialis* CFS *in vitro* (Figure S2A), was cultured overnight in TSB with 10 μg/mL trimethoprim and subcultured as described above. Cells were

Please cite this article in press as: Kowalski et al., Skin mycobiota-mediated antagonism against *Staphylococcus aureus* through a modified fatty acid, Current Biology (2025), https://doi.org/10.1016/j.cub.2025.03.055

washed and resuspended in sterile PBS. In 12 μL, ~2.5x10^7 cells were inoculated onto the surface of the skin biopsies and incubated at 37°C, 5% CO_2 for 24-h. After 24-h, control biopsies were treated with pH-matched mDixon and the test biopsies were treated with 50% CFS collected from *M. sympodialis in vitro* cultures as described above. After 24-h of treatment, the biopsies were removed and disrupted as described above to enumerate the recovered *S. aureus* CFUs/biopsy as a metric of colonization. The experiment was repeated with biopsies from four separate donors. The experiment was also repeated as just described with biopsies from a single donor with the *S. aureus* strain NRS193 (Figure S2B).

Processing of cell-free supernatant

M. sympodialis CFS was collected from 96-h monocultures as described above. The Ms-CFS was adjusted to pH 5.6 or pH 7 using HCl and NaOH. Five mLs of undiluted Ms-CFS at both pH values were separated across a 10 kDa molecular weight cutoff filter by centrifuging in a fixed-angle rotor for 5 min. at 7,000 xg per the manufacturer's protocol. The <10 kDa and >10 kDa fractions were brought to 5 mL volume with sterile water. The pH was adjusted to pH 5.5 with HCl or NaOH and filter sterilized as described above. *S. aureus* was treated with the individual fractions for 4h and CFUs were plated to enumerate survival.

For boiling experiments, 1 mL of Ms-CFS pH 5.5 or mDixon pH 5.5 were incubated at 95°C for 15 min. in the presence or absence of 1 mM DTT. *S. aureus* was exposed to the Ms-CFS or media control for 2-h as described above, and viable counts enumerated. For proteinase K treatment, 1 mL of Ms-CFS or mDixon were treated with proteinase K (500 μg/mL) for 2h at 37°C. Mock PK treatment includes exposure to buffer and incubation but in the absence of PK.

Identification of antimicrobial effector

Acid precipitation was performed by adding 0.5N HCl to static volumes of Ms-CFS or mDixon to a pH ~2.5 measured using pH indicator paper. Precipitate was pelleted by centrifugation at top speed for 5 min. at room temperature. The supernatant was decanted and readjusted to pH 5.5 and used in assays as the acid-precipitated CFS (AP-CFS) or acid-precipitated media (AP-Media). The pelleted precipitate was washed once with sterile water and resuspended in DMSO at approximately 12X. The precipitate from the Ms-CFS (CFS-P) or mDixon media (Media-P) were added back to the AP-CFS or AP-Media at 1% vol./vol. to treat *S. aureus* for 2 h and measure viability.

To identify the antimicrobial effector enriched in the CFS-P, three replicate cultures of *M. sympodialis* KS269 were grown for 96h at 30°C and the acid precipitation was performed as described above. The AP-CFS, CFS-P, Ms-CFS, mDixon (Media), AP-Media, and Media-P were prepared for analysis by LC-MS/MS as follows.

All prepared samples' MS/MS spectra were acquired using high-resolution electrospray ionization (HR-ESI) and collision-induced dissociation (CID) MS/MS with an Agilent 6550 LC-qTOF mass spectrometer coupled to an Agilent 1290 UHPLC system. Metabolites were separated on an Agilent ZORBAX Eclipse Plus C18 column (100 × 2.1 mm) under the following chromatographic conditions: 98% solvent A (0.1% formic acid in water) from 0 to 0.5 min, followed by a linear gradient to 95% solvent B (0.1% formic acid in acetonitrile) over 10 min, at a flow rate of 0.4 mL/min. A mass range of m/z 100–1700 was measured in negative ESI mode for all spectra. Data from Agilent LC-MS instruments were converted into mass spectrometry data formats compatible with SIRIUS 5 (ver. 5.8.6) dereplication tool[97] using MSConvert software.[98] Comparative analysis of the TIC chromatograms for all samples was conducted using Mzmine3 software (https://github.com/mzmine/).[99]

ATP measurements

Intracellular and extracellular ATP, iATP and eATP respectively, were quantified using the BacTiter Glo™ Microbial Cell Viability Assay. *S. aureus* was cultured in TSB as described above and adjusted to a final OD_{600}=0.1 in 5 mL of *M. sympodialis* 50% CFS or pH matched mDixon control and incubated at 37°C, 250 rpm. At 0, 15, 30, and 60 min., 1 mL aliquots were centrifuged for 1 min. at 5,000 rcf and 0.01 mL aliquots were used for serial dilutions of viable counts. The supernatant was transferred to a new tube for quantification of eATP, and cells were resuspended in mDixon for quantification of iATP. The BacTiter Glo™ reagent was prepared according to manufacturer's protocol and mixed 1:1 with the supernatant or cell suspension. Luminescence was measured using a BioTek Synergy H1 monochromator-based multi-mode microplate reader with black-walled, glass-bottom 96-well plates with 0.8s integration time per well. Luminescence for iATP was normalized to OD_{600}.

Propidium iodide staining

S. aureus NRS193 was inoculated into Ms-CFS or pH-matched mDixon media OD_{600}=0.1 and incubated at 37°C for 4-h. After, cells were centrifuged at 5000 rcf for 5 min and resuspended in 100 μL PBS with 5 μM propidium iodide. After 15 min. incubation at room temperature, cells were pelleted again and resuspended in 75 μL PBS and inoculated into black-walled, glass-bottom 96-well plates. Absorbance (OD_{600}) and fluorescence (535 nm, 617 nm) were measured using a BioTek Synergy H1 monochromator-based multi-mode microplate reader. The above protocol was repeated for 10-HP, except that cells were inoculated into AP-CFS with DMSO (vehicle) or 10-HP (25 μg/mL) for 4-h.

Serial passaging experimental evolution

S. aureus (NRS193 (WT) or HFH-29568) were cultured in TSB as described above before the OD_{600} was adjusted to 0.02 in 50% *M. sympodialis* CFS (3 populations) or pH-matched mDixon (1 population). After 8-h of exposure, a 10 μL aliquot was removed to enumerate viable counts from the four populations and the remaining volume of 190 μL was inoculated into 5 mL of TSB to facilitate

Please cite this article in press as: Kowalski et al., Skin mycobiota-mediated antagonism against *Staphylococcus aureus* through a modified fatty acid, Current Biology (2025), https://doi.org/10.1016/j.cub.2025.03.055

growth of surviving cells overnight at 37°C. The following day a portion of the recovered population was cryopreserved, the subculture in TSB to exponential phase performed as described above, and then inoculated in 50% CFS or pH-matched mDixon at OD_{600}=0.02 for 8-h. This was repeated for 12 passages. From the viable counts surviving passage 12, individual colonies were isolated and tested for their tolerance to 2-h exposure to the Ms-CFS. One representative tolerant isolate was selected from each of the Ms-CFS-exposed populations of the USA400 WT strain NRS193 (EVOL-A, EVOL-B, and EVOL-C).

S. aureus genomic DNA preparation

S. aureus genomic DNA was prepared using the Qiagen DNeasy Blood and Tissue kit with the following modifications. From a freshly inoculated TSA plate, 10-20 *S. aureus* colonies were inoculated into 0.1 mL TE buffer with 20 μg/mL lysostaphin and incubated at 37°C for 15-30 min. or until visibly cleared. The lysis buffer for Gram positive bacteria described in the DNeasy Qiagen Blood and Tissue protocol was prepared 2X and without lysozyme (40 mM Tris-HCl pH 8, 4 mM Na_2EDTA, 2.4% (v/v) triton X-100) and diluted to 1X by mixing with the lysostaphin-treated cells. The Qiagen protocol was then followed as instructed.

Whole genome sequencing and variant calling

All genome sequencing data can be accessed at the NCBI Bioproject PRJNA1107622 "*Staphylococcus aureus* strain: NRS193 Genome sequencing". Whole genome sequencing, assembly, and annotation of *S. aureus* NRS193 (GenBank: GCA_045348275.1) was performed by Plasmidsaurus. Genomic DNA was prepared as described above. Long-read sequencing was performed using Oxford Nanopore Technologies with V14 library preparation and R10.4.1 flow cells. Genome Assembly was performed using Filtlong v0.2.1, Miniasm v0.3, Flye v2.9.1, and Medaka v1.8.0. Genome annotation was performed with Bakta v1.6.1.

Genome sequencing of the evolved strains was performed using SeqCenter Illumina Whole Genome Sequencing. Genomic DNA was prepared as described above and the Illumina DNA Prep kit with bead-based tagmentation was utilized for library preparation. The Illumina sequence data (fastq) was used with the NRS193 reference genome to identify variants using *breseq* with default settings.[96]

Mupirocin treatment

S. aureus was cultured overnight in TSB and then subcultured 1:20 in TSB with 0, 1, 2, or 4 μg/mL mupirocin for 2-h. Cells were centrifuged, washed with mDixon, and inoculated into *M. sympodialis* 50% CFS or pH-matched media control with 0, 1, 2, or 4 μg/mL mupirocin at OD_{600}=0.02. After 2-h treatment, *S. aureus* cells were serially diluted to enumerate viable counts.

Bacterial growth curves

Growth curves were performed using a BioTek Synergy H1 monochromator-based multi-mode microplate reader with non-treated, sterile, polystyrene 96-well plates with lids. Unless otherwise noted, growth curves were performed for 20-h with OD_{600} measured at 10 min. intervals with incubation at 37°C and continuous orbital shaking between intervals. Each experiment included three to four technical replicates for each condition. For all conditions, *S. aureus* was inoculated at an OD_{600}=0.02. The control condition for all experiments was TSB. Oxacillin was added at 4 or 6 μg/mL and diluted from a working stock of 50 mg/mL in water. The final volume per well was 150 μL. Data was collected using the BioTek Gen5 software and analyzed in Microsoft Excel and GraphPad Prism 10. Representative curves of a minimum of three replicate experiments are shown but area under the curve (AUC) is calculated from total replicate experiments.

Genetic manipulation of *S. aureus*

For allelic replacement and in-frame deletions we generated constructs using the pIMAY system as previously described.[94] All primers used are in Table S3. Briefly, knockout constructs were generated by amplifying 500-1000bp upstream and downstream of the gene of interest. Primers P1 and P2 amplified the 5' flank and primers P3 and P4 amplified the 3' flank, where P3 includes homology to P2. Overlap extension PCR with primers P5 and P6 set ~100 bp inside of P1 and P4, respectively, was performed to stitch together the flanks. For the *rel* allele swaps, the allele of interest was amplified from genomic DNA using Rel_swap_P1 and Rel_swap_P2 primers. PCR fragments and the fused construct were column purified. The purified construct was phosphorylated with T4 polynucleotide kinase according to the manufacturer's protocol. pIMAY, purchased from Addgene, was prepared from *E. coli* DH5a using the ZymoPure II Plasmid Midiprep kit, digested with SmaI, and treated with shrimp alkaline phosphatase according to the manufacturer's protocol. The purified fusion construct was ligated into SmaI-digested pIMAY with Quick Ligation Kit and transformed into chemically competent *E. coli* DC10B.[94] Colonies were isolated on 25 μg/mL chloramphenicol and the insertion into pIMAY confirmed with primers IM51 and IM51. Confirmed plasmids were midi-prepped from a 100 mL culture as described above and further concentrated using Novagen Pellet Paint Co-precipitant.

Electrocompetent *S. aureus* strains were generated as previously described[101] and transformed with ~5 μg of the pIMAY construct using the BioRad Gene Pulser Xcell electroporation system and 1 mm disposable electroporation cuvettes. The pulse was 21kV/cm, 100 Ω, and 25 mF and cells were immediately resuspended in 1 mL of TSB + 500 mM sucrose and incubated at 28°C or 30°C for 1-2-h before plating on TSA with 10 μg/mL chloramphenicol and incubating at 28°C for 48-h. Large colonies were resuspended in 500 μL of TSB and 10 μL streaked on a new TSA plate with 10 μg/mL chloramphenicol and incubated at 37°C overnight to initiate integration onto the chromosome. Large colonies were screened with colony PCR for integration through the 5' flank using primers P1 and P6. Positive colonies were grown overnight at 28°C in TSB without antibiotic and then subcultured 1:10 in TSB with 1 μg/mL anhydrotetracycline hydrochloride (aTC) at 28C for ~6-h before 10 μL was quadrant streaked on a TSA plate with 1 μg/mL aTC and incubated at

Please cite this article in press as: Kowalski et al., Skin mycobiota-mediated antagonism against *Staphylococcus aureus* through a modified fatty acid, Current Biology (2025), https://doi.org/10.1016/j.cub.2025.03.055

28°C for 48-h. Single colonies were patched on TSA with 1 μg/mL aTC or TSA with 10 μg/mL chloramphenicol. Only colonies that grew on aTC and not chloramphenicol were screened for gene deletion with internal primers and P1 and P4.

For the introduction of the natural *rel* variants, the construct generated above with the WT *rel* allele in pIMAY (pRel-swap) was used for site directed mutagenesis with the Q5-Site-Directed-Mutagenesis kit according to the manufacturer's instruction. The mutagenesis primers were designed using the NEBaseChanger version 1.3.3. Mutagenesis was confirmed with either whole plasmid sequencing or Sanger sequencing. Mutated plasmids were transformed into *E. coli* DC10B and *S. aureus* as described above. Allele replacement was confirmed with Sanger sequencing in *S. aureus*.

For generation of Pasp23-YFP reporter strains, the promoters were amplified from *S. aureus* genomic DNA with primers Pasp23 P1 and P2 (Table S3). PCR products were column purified and digested with EcoRV and XbaI according to the manufacturer's protocol. Plasmid pTH3 was also digested with EcoRV and XbaI and treated with rSAP. The amplified promoters were ligated into pTH3 replacing the original promoter upstream of YFP with Quick Ligation and transformed into *E. coli* DC10B. To integrate the reporter on the chromosome, we opted to use a neutral site previously reported for the integration of fluorescent proteins in *S. aureus* MW2.[95] The promoter-YFP-terminator constructs were amplified from modified pTH3 with primers rep_chr_p1 and rep_chr_P2. The flanks at the integration site were amplified from genomic DNA with rep_chr_P3 and rep_chr_P4 for one flank and rep_chr_P5 and rep_chr_P6 for the other flank. The flanks and promoter-YFP construct were stitched together through overlap extension PCR with primers rep_chr_P7 and rep_chr_P8. As described above for the deletion constructs, the reporter constructs with flanks were phosphorylated and ligated into pIMAY before transformation into *E. coli* DC10B. The transformation of *S. aureus* was the same as described above.

Identification of natural Rel alleles

To identify natural Rel alleles that resemble those in the Ms-CFS-derived tolerant strains, we queried the NCBI Identical Proteins Database. We used 'GTP pyrophosphokinase' as the search term and *Staphylococcus aureus* as the organism. To eliminate sequences corresponding to RelP and RelQ, we limited our results to a sequence length between 300 and 1000 amino acids. This resulted in 283 unique protein sequences. Based on the methionine annotated as the start codon, the majority of Rel sequences are 729 or 736 amino acids in length. All 283 FASTA files were downloaded and aligned in SnapGene. Two sequences were excluded that appeared to be misannotated as *S. aureus*. We focused on alleles with C-terminal truncations and compiled those in Table S2. These truncated alleles have one or two genomes corresponding to each sequence. Following this query, a study was published where C-terminal mutations like those observed in the CFS-derived strains were observed in clinical isolates.[55]

MIC and time-kill assays

Minimum inhibitory concentration for oxacillin were determined following protocols previously described.[48] Briefly, *S. aureus* grown overnight in TSB and subcultured to exponential phase were inoculated into 0-128 μg/mL oxacillin at 2-fold dilutions at an initial OD_{600}=0.02 in a 96-well plate. The final volume per well was 200 μL. After 24-h at 37°C, the minimum inhibitory concentration is reported as range from the highest concentration where *S. aureus* grows to the lowest concentration where there is no growth.

Time-kill assays were performed as previously described.[48] Briefly, *S. aureus* was grown overnight in Mueller-Hinton Broth (MHB) and subcultured 1:10 for 1-h at 37°C in the same media. *S. aureus* was inoculated into MHB with the following antibiotics: 1 μg/mL vancomycin, 100 μg/mL daptomycin, or 0.5 μg/mL ciprofloxacin. These antibiotics were selected because they had previously been shown to have reduced activity against *S. aureus* expressing the F128Y Rel allele in contrast to other antibiotics that had no differences in sensitivity.[48] Aliquots were taken at 0, 1, 2, 4, 6, and 8-h as necessary to enumerate *S. aureus* viable counts by serial dilution and plating on TSA. The minimum duration of killing was calculated for each independent experiment using the data points within the linear range and applying the linear regression and interpolation functions in GraphPad Prism as previously described.[48]

Quantification of pppGpp

S. aureus strains were grown overnight in low-phosphate chemically defined media (CDM)[102] at 37°C. Cultures were diluted to an OD_{600} of 0.1 and grown for 2-h prior to the addition of 3.7 MBq of [^{32}P]H_3PO_4 and incubation for a further 3-h at 37°C. Cultures were subsequently normalized for absorbance and to one set the stringent response was induced by the addition of 60 μg/mL mupirocin. Cells were incubated at 37°C for 30 min, before being recovered by centrifugation (17,000 rcf for 5 min) and suspended in 100 μL of 2M formic acid. Cells were subjected to three freeze/thaw cycles and debris removed by centrifugation (17,000 rcf for 5 min) before the lysate was filtered through a 3 kDa spin column. Ten microliters were subsequently spotted on PEI-cellulose F thin-layer chromatography (TLC) plates, nucleotides separated, and TLC plates developed using a 1.5 M KH_2PO_4 pH 3.6 buffer. The radioactive spots were visualized using an FLA 7000 Typhoon PhosphorImager, and data were quantified using ImageQuant TL software.

QUANTIFICATION AND STATISTICAL ANALYSIS

Statistical analyses were performed using Prism 10 (GraphPad). Figure legends include details on statistical test, sample number, donor number, and *p* value. *p* values: $p >/= 0.05$ not significant (ns), $p<0.05$ (*), $p<0.01$ (**), $p<0.001$ (***), $p<0.0001$ (****). For all graphs the center indicates the mean and error bars indicate SEM.